

6.

Determination of the optimal constant output feedback gains applied to the control of a deck-wings system

The optimal control of time-invariant systems with respect to a quadratic performance criterion is developed next. The problem is posed with the additional constraint that the control vector $\mathbf{u}(t)$ is a linear time-invariant function of the output vector $\mathbf{y}(t)$ rather than of the state vector $\mathbf{x}(t)$. This formulation has been chosen in the case of control of the present deck-wings system because it is desirable to generate the control variables directly by taking linear combinations of the available output variables. As the original system is time invariant and the linear combinations are also constrained to be time-invariant, the design problem is to choose an appropriate matrix of feedback gains \mathbf{K} .

6.1. Formulation

The optimization problem begins with a time-invariant linear system, whose state vector $\mathbf{x}(t)$, control vector $\mathbf{u}(t)$ and output vector $\mathbf{y}(t)$ are related by [103]:

$$\dot{\mathbf{x}}(t) = \mathbf{A} \mathbf{x}(t) + \mathbf{B} \mathbf{u}(t) \quad (6.1a)$$

$$\mathbf{y}(t) = \mathbf{C} \mathbf{x}(t) \quad (6.1b)$$

\mathbf{A} state matrix (14x14) in the present case;

\mathbf{B}_u matrix affecting the signal $\mathbf{u}(t)$;

$\mathbf{x}(t)$ state vector (14 x 1) in the present case;

$\mathbf{u}(t) = \begin{bmatrix} u_1 \\ u_2 \end{bmatrix}$ control vector (signal);

$\mathbf{y}(t)$ output vector(6 x 1) in the present case;

\mathbf{C} [6x8] matrix, relating the output vector $\mathbf{y}(t)$ to the structural states of the state vector $\mathbf{x}(t)$.

The vector \mathbf{B}_u reads (see equation 5.26):

$$\mathbf{B}_u = \begin{bmatrix} \mathbf{M}_s^{-1} \mathbf{B}_s \\ 0 \\ 0 \end{bmatrix} = \begin{bmatrix} 0 & 0 \\ 0 & 0 \\ \omega_d^2 & 0 \\ 0 & \omega_d^2 \\ 0 & 0 \\ 0 & 0 \\ 0 & 0 \\ 0 & 0 \\ 0 & 0 \\ 0 & 0 \\ 0 & 0 \\ 0 & 0 \\ 0 & 0 \\ 0 & 0 \end{bmatrix} \quad (6.2)$$

The output vector \mathbf{y} is a vector representing system physical properties that can be measured by electronic devices and used for feedback purposes, as the deck heave velocity \dot{h}/B , the pitch velocity $\dot{\alpha}$, the deck heave h/B , and pitch α and the winglet rotations δ_1 and δ_2 . The angular velocity of the winglets was not selected for feedback purposes.

The control must result in small wing pitches. Ostenfeld & Larsen [53] propose to vary the angle of rotation of the winglets in time as a predetermined function of the angle of rotation of the girder, so that if the bridge is rotating in a sinusoidal motion at a frequency ω , the flap is rotating at the same frequency but out of phase, as given by:

$$\text{Deck rotation: } \alpha(t) = \alpha_0 \sin(\omega t)$$

$$\text{Winglet rotation: } \delta_\omega(t) = \nu \alpha_0 \sin(\omega t + \psi)$$

where ν controls the amplitude of the winglet and ψ is the out-of-phase angle between the movement of the flap and the movement of the girder. These two parameters (ν , ψ) govern the movement of the flap and must be defined by the designer. The suggested maximum angle of rotation for the winglet is about 15° (a maximum angle of rotation must be imposed to avoid flow separation in the winglet). Thinking in terms of a maximum rotation angle for the deck on the order of, say 5° , this leaves ψ to vary in the range of $0 < |\psi| < \pi$.

The approach followed by Ostenfeld & Larsen [53] differs from Wilde & Fujino [96] in the sense that the law of movement of the control surfaces is prescribed, instead of explicitly addressing the control of winglets using active control theory.

However, low absolute values for the angle of rotation of the winglets (δ_1 and $\delta_2 < 15^\circ$) seem reasonable whichever version is applied. The matrix \mathbf{C} relating the output vector \mathbf{y} to the structural states of the state vector \mathbf{x} is:

$$\begin{bmatrix} y1 \\ y2 \\ y3 \\ y4 \\ y5 \\ y6 \end{bmatrix} = \begin{bmatrix} 1 & 0 & 0 & 0 & 0 & 0 & 0 \\ 0 & 1 & 0 & 0 & 0 & 0 & 0 \\ 0 & 0 & 0 & 0 & 1 & 0 & 0 \\ 0 & 0 & 0 & 0 & 0 & 1 & 0 \\ 0 & 0 & 0 & 0 & 0 & 0 & 1 \\ 0 & 0 & 0 & 0 & 0 & 0 & 1 \end{bmatrix} \begin{bmatrix} \dot{h}/B \\ \dot{\alpha} \\ \dot{\delta}_1 \\ \dot{\delta}_2 \\ h/B \\ \alpha \\ \delta_1 \\ \delta_2 \end{bmatrix} \quad (6.3)$$

└──────────────────┘

C

The optimal control of the time-invariant system is performed with respect to a quadratic performance criterion, as proposed by Levine and Athans [41]. The problem is posed with the additional constraint that the control vector $\mathbf{u}(t)$ is a linear time-invariant function of the output vector $\mathbf{y}(t)$ or :

$$\mathbf{u}(t) = -\mathbf{K} \mathbf{y}(t) \quad (6.4)$$

rather than of the state vector $\mathbf{u}(t)$. Following Levine and Athans, and as a first try at a reasonable performance measure, the following standard infinite time quadratic performance criterion is applied :

$$J_t = \frac{1}{2} \int_0^{\infty} \{ \mathbf{x}(t)' \mathbf{Q} \mathbf{x}(t) + \mathbf{u}(t)' \mathbf{R} \mathbf{u}(t) \} dt \quad (6.5)$$

Equations (6.1) and (6.5) form an optimization problem for which the optimal control can be generated by $\mathbf{u}(t) = \mathbf{G} \mathbf{x}(t)$. The feedback matrix can be evaluated through the solution of an algebraic Riccati's equation, (see Ogata [50], item 12-8 - Quadratic Optimal Regulator Systems, for a deduction of the Riccati equation applied to the minimization of $J_t = \frac{1}{2} \int_0^{\infty} \{ \mathbf{x}(t)' \mathbf{Q} \mathbf{x}(t) + \mathbf{u}(t)' \mathbf{R} \mathbf{u}(t) \} dt$. See also MATLAB's subroutine "LQR" which returns the feedback matrix \mathbf{G} of a system consisting of matrices \mathbf{A} , \mathbf{B} , \mathbf{Q} , \mathbf{R} by using the MATLAB command: "[G, S, e] = lqr (A, B, Q, R, N)".

The present problem is different, though. Suppose that one introduces the constraint that the control $\mathbf{u}(t)$ is generated via output linear feedback gains, i. e.:

$$\mathbf{u}(t) = -\mathbf{K} \mathbf{y}(t) \quad (6.6)$$

$$\mathbf{u}(t) = -\mathbf{K} \mathbf{C} \mathbf{x}(t) \quad (6.7)$$

where \mathbf{K} is the feedback gains matrix to be determined.

Under this constraint, the system (6.1), (6.2) can be rewritten as

$$\dot{\mathbf{x}}(t) = [\mathbf{A} - \mathbf{B} \mathbf{K} \mathbf{C}] \mathbf{x}(t) \quad (6.8)$$

where $[A - B K C]$ is the closed loop matrix. It should be clear that K is regarded as the control for the system (6.8). In addition, $x(t)$ is given by:

$$x(t) = \Phi(t, 0) \cdot x(0) \quad (6.9)$$

where $\Phi(t, 0)$ is the fundamental transition matrix for the system (6.9) and

$$\Phi(t, 0) = e^{[A - B K C]t}$$

Substituting (6.9) in the performance criterion (6.5), gives:

$$J = x(0)' \left[\frac{1}{2} \int_0^{\infty} [\Phi(t, 0)' (Q + C' K' R K C) \Phi(t, 0)] dt \right] x(0) \quad (6.10)$$

Equation (6.10) emphasizes the dependence of the performance criterion on both K (the control) and $x(0)$ (the initial state). In order to use the performance criterion to find an optimal feedback control K , it is usually necessary to eliminate this dependence on the initial state. Mathematically, a simple way to eliminate the dependence on the initial state is to average the performance obtained for a linearly independent set of initial states. This is equivalent to assuming the initial state $x(0)$ to be a random variable uniformly distributed on the surface of the n -dimensional unit sphere. Then, the expected value of the performance criterion J is, according to Levine and Athens:

$$\hat{J} = \frac{1}{2n} \int_0^{\infty} \text{tr} [\Phi(t, 0)' (Q + C' K' R K C) \Phi(t, 0)] dt \quad (6.11)$$

Norlander et al. [49] apply the same procedure to a problem of the aerospace industry.

This average performance \hat{J} is independent of the initial state. Equation (6.11) can also be interpreted as a completely deterministic performance criterion in which the control is K and the state is $\Phi(t, 0)$, the fundamental transition matrix.

6.2. Statement of the optimization problem

The following optimization problem is considered: Given the time-invariant linear system

$$\dot{\Phi}(t, 0) = [A - B K C] \Phi(t, 0), \quad \Phi(0, 0) = I \quad (6.12)$$

It is well known that

$$\Phi(t, 0) = \exp ([A - B K C] t) \quad (6.13)$$

Given the performance criterion (the constant $1/n$ has been dropped)

$$\hat{J} = \int_0^{\infty} \text{tr} [\Phi(t, 0)' (\mathbf{Q} + \mathbf{C}' \mathbf{K}' \mathbf{R} \mathbf{K} \mathbf{C}) \Phi(t, 0)] dt \quad (6.14)$$

find that \mathbf{K} which minimizes the performance criterion (6.14) subject to the constraint imposed by the system (6.6). For the sake of completeness:

A $n \times n = (14 \times 14)$, where $n =$ number of states

B $n \times m = (14 \times 2)$

C $r \times p = (6 \times 8)$, where r is the rank of the output variables ($= 6$)

Q $p \times p = (8 \times 8)$, a symmetric positive semi definite real constant matrix. Here \mathbf{Q} is a diagonal matrix where p is the number of structural states.

R $m \times m = (2 \times 2)$ = a diagonal matrix, where $m =$ number of controls, here the controls on the 2 wings.

K $m \times r = (2 \times 6)$, a real and stable matrix.

Note that the size of vectors and matrices are specific to the problem under consideration and 2 lag terms for the deck and wings.

6.3. The main result

The major result arrived at by Levine and Athans is summarized in the following theorem:

Let \mathbf{K}^* be a real constant $m \times r$ (2×6) matrix. Let

$$\mathbf{A}_c = [\mathbf{A} - \mathbf{B} \mathbf{K} \mathbf{C}] \quad (6.15)$$

Assuming that \mathbf{A}_c is stable, then, in order for \mathbf{K}^* to be optimal it is necessary that $\left. \frac{dJ}{d\mathbf{K}} \right|_{\mathbf{K}^*} = 0$.

which is equivalent to the equation:

$$\mathbf{K}^* = \mathbf{R}^{-1} \mathbf{B}' \mathbf{P} \mathbf{L} \mathbf{C}' [\mathbf{C} \mathbf{L} \mathbf{C}']^{-1} \quad (6.16)$$

where

$$\mathbf{P} \cong \int_0^{\infty} \exp(\mathbf{A}'_c \tau) [\mathbf{Q} + \mathbf{C}' \mathbf{K}^{*'} \mathbf{R} \mathbf{K}^* \mathbf{C}] \exp(\mathbf{A}_c \tau) d\tau \quad (6.17)$$

$$\mathbf{L} \cong \int_0^{\infty} \exp(\mathbf{A}_c \sigma) \exp(\mathbf{A}'_c \sigma) d\sigma \quad (6.18)$$

where $\exp(\mathbf{A}_c \sigma) = e^{(\mathbf{A}_c \sigma)}$ and $\exp(\mathbf{A}'_c \tau) = e^{(\mathbf{A}'_c \tau)}$

Alternatively, assuming that $\mathbf{P}, \mathbf{L}, \mathbf{K}^*$ are solutions of (6.16) to (6.18) then \mathbf{P} is also a positive semi definite solution of

$$\mathbf{P}\mathbf{A}_c + \mathbf{A}'_c\mathbf{P} + \mathbf{Q} + \mathbf{C}'\mathbf{K}^*\mathbf{R}\mathbf{K}^*\mathbf{C} = \mathbf{0} \quad (6.19)$$

And \mathbf{L} is a positive definite solution of

$$\mathbf{L}\mathbf{A}'_c + \mathbf{A}_c\mathbf{L} + \mathbf{I} = \mathbf{0} \quad (6.20)$$

The derivation of the results above can be found in Levine and Athans [41]. The solution of (6.16), (6.19) and (6.20) is obtained in the iterative way by the following steps:

Start with a stable initial gain \mathbf{K}^* .

Substitute \mathbf{K}^* in equation (6.19). All variables are known but \mathbf{P} . Hence, \mathbf{P} is determined, (6.19) being a Sylvester equation of the type $\mathbf{A}\mathbf{X} + \mathbf{X}\mathbf{B} + \mathbf{Z} = \mathbf{0}$, where $\mathbf{A}\mathbf{X} = \mathbf{A}_c\mathbf{L}$, $\mathbf{X}\mathbf{B} = \mathbf{L}\mathbf{A}'_c$, $\mathbf{Z} = \mathbf{Q} + \mathbf{C}'\mathbf{K}^*\mathbf{R}\mathbf{K}^*\mathbf{C}$.

Substitute \mathbf{K}^* in equation (6.20) . All variables are known but \mathbf{L} . Hence, \mathbf{L} can be determined, (6.20) being a Lyapunov equation of the type $\mathbf{X}\mathbf{A}' + \mathbf{A}\mathbf{X} + \mathbf{Z} = \mathbf{0}$

Find a new \mathbf{K}^* by entering \mathbf{P} and \mathbf{L} in (6.16).

The Lyapunov and Sylvester equations can be solved with the MATLAB program called “ lyap “, which solves the special and general forms of the Lyapunov matrix equation.

The command “ $\mathbf{X} = \text{lyap}(\mathbf{A}, \mathbf{Z})$ “ solves the Lyapunov equation $\mathbf{X}\mathbf{A}' + \mathbf{A}\mathbf{X} + \mathbf{Z} = \mathbf{0}$ where \mathbf{A} and \mathbf{Z} are square matrices of identical sizes. The solution \mathbf{X} is a symmetric matrix if \mathbf{Z} is one.

The command “ $\mathbf{X} = \text{lyap}(\mathbf{A}, \mathbf{B}, \mathbf{Z})$ “ solves the Lyapunov equation $\mathbf{A}\mathbf{X} + \mathbf{X}\mathbf{B} + \mathbf{Z} = \mathbf{0}$ The matrices \mathbf{A} , \mathbf{B} , \mathbf{Z} must have compatible dimensions but need not be square.

The MATLAB program “ lqr ” is called by the main program to solve the Lyapunov-type equations and perform the optimization of $\mathbf{K}^* \rightarrow \mathbf{K}^*_{\text{opt}}$ through loop commands and tolerance settings. The main difficulty in these procedures is to define a stable initial gain matrix \mathbf{K}^* in order to obtain the optimum $\mathbf{K}^*_{\text{opt}}$.

According to Levine and Athans [41], the following lemma provides the basis for a computer algorithm which may converge to \mathbf{K}^* .

Let

$$\mathbf{P}_n[\mathbf{A} - \mathbf{B}\mathbf{K}_{n-1}\mathbf{C}] + [\mathbf{A} - \mathbf{B}\mathbf{K}_{n-1}\mathbf{C}]'\mathbf{P} + \mathbf{Q} + \mathbf{C}'\mathbf{K}_{n-1}'\mathbf{R}\mathbf{K}_{n-1}\mathbf{C} = \mathbf{0} \quad (6.22)$$

$$\mathbf{L}_{n-1}[\mathbf{A} - \mathbf{B}\mathbf{K}_{n-1}\mathbf{C}]' + [\mathbf{A} - \mathbf{B}\mathbf{K}_{n-1}\mathbf{C}]\mathbf{L}_{n-1} + \mathbf{I} = \mathbf{0} \quad (6.23)$$

Then, assuming that $\mathbf{Q} > \mathbf{0}$ and $[\mathbf{A} - \mathbf{BK}_{n-1}\mathbf{C}]$ are stable, a unique and positive definite \mathbf{K}_n exists. Furthermore, assuming there exists a positive definite \mathbf{L}_{n-1} which satisfies equation (6.23), then $\text{trace}[\mathbf{P}_n] \leq \text{trace}[\mathbf{P}_{n-1}]$, where $\text{trace}[\mathbf{P}_n]$, $\text{trace}[\mathbf{P}_{n-1}]$, are the sum of the diagonal elements of the matrices \mathbf{P}_n , \mathbf{P}_{n-1} . The lemma does not prove that the algorithm will converge. It only shows that \mathbf{P}_n is better than \mathbf{P}_{n-1} provided that some fairly strong hypotheses are satisfied.

6.4. Applications for aerodynamic control

$$\underbrace{\begin{bmatrix} \ddot{\mathbf{q}} \\ \dot{\mathbf{q}} \\ \dot{\mathbf{x}}_a \end{bmatrix}}_{\dot{\mathbf{x}}} = \underbrace{\begin{bmatrix} \mathbf{M}_s^{-1}(-\mathbf{C}_s + \mathbf{S} \mathbf{A}_1^s) & \mathbf{M}_s^{-1}(-\mathbf{K}_s + \mathbf{S} \mathbf{A}_0^s) & \mathbf{M}_s^{-1} \mathbf{D}_s \\ \mathbf{I} & \mathbf{0} & \mathbf{0} \\ \mathbf{0} & \mathbf{G}_s & -\mathbf{F}_s \end{bmatrix}}_{\mathbf{A}} \underbrace{\begin{bmatrix} \dot{\mathbf{q}} \\ \mathbf{q} \\ \mathbf{x}_a \end{bmatrix}}_{\mathbf{x}} + \underbrace{\begin{bmatrix} \mathbf{M}_s^{-1} \mathbf{B}_s \\ \mathbf{0} \\ \mathbf{0} \end{bmatrix}}_{\mathbf{B}_u} \mathbf{u} + \underbrace{\begin{bmatrix} \mathbf{M}_s^{-1} \mathbf{B}_s \\ \mathbf{0} \\ \mathbf{0} \end{bmatrix}}_{\mathbf{B}_{buf}} \mathbf{F}_{buf} \quad (6.24)$$

The Matrix \mathbf{A} in the equation (6.24) is a function of mean wind speed. Thus, application of the conventional output feedback design requires in the first place the selection of a design wind velocity U_d , then computation of the system matrix for this U_d and determination of the associated gain matrix \mathbf{K} . Finally, the performance of the controller can be verified for the desired range of wind velocities.

The geometrical and dynamic characteristics as well as the rational model of unsteady forces due to structural motions in the fluid are consistent with the parameters given in the previous section. The chord length of the control surfaces corresponds to 10% of the bridge deck width, and the position of the surfaces is chosen as $e_1 = e_2 = B/2$ in Figure 5-1.

The dynamic characteristics of the equation governing the relative motion of the control surfaces due to the control signal $\mathbf{u}(t)$ are selected as $f_\delta = 6$ Hz and $\xi_\delta = 70\%$. The measurements available for feedback are chosen as:

$$y = \begin{bmatrix} \dot{h}/B \\ \dot{\alpha} \\ h/B \\ \alpha \\ \delta_1 \\ \delta_2 \end{bmatrix} \quad (6.25)$$

The variation of the open-loop system properties, i.e., modal frequencies and damping ratios with wind speed for the deck-wing system without control is presented in item 5.3. The flutter wind speed corresponds to the point where the damping of the dominant mode (the pitching) becomes null. This occurs for the wind speed $U_{crit} = 10.663$ m/s, as shown in Chapter 5. Note that the flutter wind speed of the deck with stationary control surfaces is about 5 % higher compared to the deck alone (without wings), equal to 10.2 m/s. At the flutter wind velocity, the frequencies of heaving and pitching modes of the system with stationary wings become almost identical, as in the classical case of flutter of two degrees of freedom systems. For the increase of wind speed beyond U_{crit} , the damping of pitching mode decreases markedly and the bridge becomes highly unstable.

The geometrical and dynamic characteristics of the deck-wind system correspond to a section model of Akashi Strait Bridge, in the scale 1:150, as reported by Wilde & Fugino [96]. The mass matrix was not mentioned there, but could be deduced from equation (28) of this same article.

6.5. Closed-loop systems

The objective of the control design for this bridge model with active surfaces is to suppress flutter up to a wind velocity of 21 m/s.

The feedback gain matrix \mathbf{K} and the closed-loop eigenvalues and eigenvectors are determined by the optimization criterion:

$$J_t = \frac{1}{2} \int_0^{\infty} \{ \mathbf{x}(t)' \mathbf{Q} \mathbf{x}(t) + \mathbf{u}(t)' \mathbf{R} \mathbf{u}(t) \} dt \quad (6.25)$$

or, in other words, by choice of the matrices \mathbf{Q} on the state vector and \mathbf{R} on the controls signals. The variation of weights \mathbf{R} on the control signals are assumed to be:

$$\mathbf{R} = [\rho_r(U_d)] \mathbf{I} \quad (6.26)$$

where \mathbf{I} is the identity matrix [2x2] and $[\rho_r(U_d)]$ is a scalar constant adjusted for each U_d . If ρ_r is large, the control gains achieve their smallest possible magnitudes and so the utilized magnitude of relative motion of the surfaces is

small. Small motions of the control surfaces are one of the desired properties of the feedback control, as already mentioned. Formula (6.27) assumes equal weights on both leading and trailing surfaces. Thus, the resulting gain tends to keep the same magnitude of relative motion of both wings. One must remember that the adequate wing pitch is limited to 15° , as already pointed out in item 6.1.

The weighing matrix \mathbf{Q} on the state vector is a diagonal matrix with constant coefficients. The first four diagonal terms are assigned to velocities and the next four diagonal terms to displacements, i.e., to the components of the state vector.

The selection of weights for different design velocities can be simplified by varying the weight ρ_r over the displacement of the heaving mode alone. The deck mass and stiffness matrices are chosen as the terms of the \mathbf{Q} matrix because part of the minimization of the performance index J is in fact the minimization of $\mathbf{x}' \mathbf{Q} \mathbf{x}$ (or the minimization of kinetic energy $\frac{1}{2} m.v^2$) plus the minimization of $(\mathbf{K}\delta)' \mathbf{R} \delta$ (or the minimization of work done by stiffness forces $\frac{1}{2} (k \cdot \delta) \cdot \delta$), or, in matrix form:

$$\frac{1}{2} \begin{bmatrix} \dot{h}/B & \dot{\alpha} \end{bmatrix} \begin{bmatrix} mB & 0 \\ 0 & I_\alpha \end{bmatrix} \begin{bmatrix} h/B \\ \alpha \end{bmatrix} \quad (6.27a)$$

which is a kinetic energy, plus

$$\frac{1}{2} \begin{bmatrix} h/B & \alpha \end{bmatrix} \begin{bmatrix} k_h B & 0 \\ 0 & k_\alpha \end{bmatrix} \begin{bmatrix} h/B \\ \alpha \end{bmatrix} \quad (6.27b)$$

which is the work done by the stiffness forces.

Hence, in order to obtain a consistent gains matrix for a chosen wind velocity, the terms $Q_i, i=1,2,3,4,5,6,7,8$ are chosen as follows:

$$\mathbf{Q} = \text{diag. matrix } [mB \quad I_\alpha \quad I_\delta \quad I_\delta \quad \rho_q(k_h B) \quad k_\alpha \quad k_w B_w \quad k_w B_w]$$

Note that the aerodynamic terms were discarded, because no controls are assigned to them. By the same token, the I_δ and $k_w B_w$ terms can also be discarded, leaving:

$$\mathbf{Q} = \text{diag. matrix } [mB \quad I_\alpha \quad 0 \quad 0 \quad \rho_q(k_h B) \quad k_\alpha \quad 0 \quad 0]$$

Substituting $mB = 0.559$, $I_\alpha = 0.00191$, $k_h B = 3.4707$ $k_\alpha = 1.21462$ in the equation above, equation (6.28a) is obtained:

$$\mathbf{Q} = \text{diag. matrix } [0.559 \quad 0.00191 \quad 0 \quad 0 \quad \rho_q(3.4707) \quad 1.21462 \quad 0 \quad 0]$$

Another choice for \mathbf{Q} would be to vary the weight ρ_q over the pitching mode exclusively. Then, matrix \mathbf{Q} would be selected as in equation (6.28b) below:

$$Q = \text{diag. matrix} [0.559 \quad 0.00191 \quad 0 \quad 0 \quad 3.4707 \quad \rho_q(1.21462) \quad 0 \quad 0]$$

From a preliminary point of view, this choice would be hardly better than the previous one, because the lifting forces on the wings tend to stabilize the torsion of the deck, while they have little effect on the heaving displacements. Thus, putting weight on pitching would probably not increase the flutter velocity.

The computation of gains was performed for several wind velocities included in the design range from 9 to 21 m/s. The features of the control laws determined for different values of U_d can be explained by analyzing gains associated with wind speed close to the flutter velocity, namely $\rho_q = 11$ m/s, and gain designed for high wind speed, $U_d = 19$ m/s. The numerical values of these gains are shown below. Matrices \mathbf{K} for $U_d = 11$ m/s and \mathbf{K} for $U_d = 19$ m/s are printed in [96], while \mathbf{K} for $U_d = 9$ m/s and \mathbf{K} for $U_d = 15$ m/s were taken from Wilde [95].

$$\mathbf{K}^{U_d=9 \text{ m/s}} = \begin{bmatrix} -0.093 & 0.094 & -0.377 & 0.420 & 0.461 & -0.250 \\ 0.019 & -0.045 & 0.114 & 0.188 & -0.222 & 0.155 \end{bmatrix} \quad (6.29)$$

$$\mathbf{K}^{U_d=11 \text{ m/s}} = \begin{bmatrix} -0.076 & 0.116 & -0.576 & 0.758 & 0.569 & -0.005 \\ 0.044 & -0.086 & 0.380 & -0.222 & -0.443 & 0.124 \end{bmatrix} \quad (6.30)$$

$$\mathbf{K}^{U_d=15 \text{ m/s}} = \begin{bmatrix} -0.011 & 0.140 & -0.322 & 1.687 & 1.052 & -0.042 \\ -0.018 & -0.081 & 0.221 & -0.794 & -0.357 & -0.050 \end{bmatrix} \quad (6.31)$$

$$\mathbf{K}^{U_d=19 \text{ m/s}} = \begin{bmatrix} -0.062 & 0.172 & -0.386 & 3.721 & 2.349 & 0.034 \\ -0.019 & -0.095 & 0.243 & -1.349 & -0.605 & 0.114 \end{bmatrix} \quad (6.32)$$

The next figures show the variation of the damping ratio and mode frequencies of the closed-loop system with gain designed for $U_d = 9$, $U_d = 11$, $U_d = 15$, $U_d = 19$ m/s as a function of wind speed. The associated ρ_q and ρ_r are :

For $U_d = 9$ m/s	$\rho_q = 1$	$\rho_r = 5$
For $U_d = 11$ m/s	$\rho_q = 5$	$\rho_r = 30$
For $U_d = 15$ m/s	$\rho_q = 10$	$\rho_r = 300$
For $U_d = 19$ m/s	$\rho_q = 20$	$\rho_r = 500$

(6.33)

The changes of damping ratios in these cases are comparable to the variations of the damping factors in the open-loop system. Instability occurs when the damping ratio of either the pitching or the heaving mode becomes negative for the following velocities:

For $U_d = 9$ m/s	$U_{crit} = 11.9$ m/s
For $U_d = 11$ m/s	$U_{crit} = 12.7$ m/s
For $U_d = 15$ m/s	$U_{crit} = 23.0$ m/s
For $U_d = 19$ m/s	$U_{crit} = 30.7$ m/s

(6.34)

6.6. Results

6.6.1. Analysis of the plots of frequencies and damping ratios

The state matrix $A_c = A - BKC$ is assembled for increasing wind velocities. The eigenvalues, damping ratios and frequencies are determined for the assemble state matrix, until the critical velocity is reached and beyond. Plots of the damping ratios and frequencies versus wind velocities are drawn. The critical velocity, the state matrix assembled with the critical velocity, as well as its eigenvalues, damping ratios and frequencies, are printed.

In order to define which mode causes the instability of the controlled structure, plots of damping ratios and frequencies can be consulted in conjunction with the computer output, according to the following explanations. By definition, the damping ratios are $\xi_h = 0.0011$ (heaving) and $\xi_\alpha = 0.010$ (pitching) at $t = 0$. Hence, after $t = 0$, the ξ_h curve runs always above ξ_α , as in the open loop system. (cf. Figure 5-3) Likewise, the initial pitching and heaving frequencies are known. Hence, the entire trajectory of ξ_h , ξ_α and ω_h , ω_α can be traced from $U = 0$ to the end of the curves of damping ratios and frequencies versus wind velocity, including the domain close to the critical velocity.

The mode that reaches instability is the one whose damping ratio crosses the ξ axis from a positive to a negative value. Once the mode of interest is identified, the computer output is consulted to complement the analysis of the plots. The state matrix A_c for the critical velocity of 30.67 m/s, shown in Table 6-7, is taken as example. A complex eigenvalue analysis of the state matrix A_c is performed by the MATLAB subroutine [Ome,Ksi] = damp (Ac). Its 14 eigenvalues and the corresponding frequencies and damping ratios are shown in the first three columns of Table 6-8. The eigenvalue and the frequency corresponding to zero

damping ratios are respectively $3.11e-004+4.44e+001i$ and 44.4 rad/s. The eigenvalue, damping ratio and frequency of the second mode of interest are $-7.66e-001+1.14e+001i$, 0.00671 and 11.4 rad/s.

With this information available, the trajectory of damping ratios and frequencies of heaving and pitching can be identified in the plots, for all four cases in question.

In order to calculate the amplitudes $h = h_0 e^{i\omega t}$ and $\alpha = \alpha_0 e^{i(\omega t + \varphi)}$ and the phase difference φ , the diagonal matrix of the eigenvalues and the corresponding eigenvectors must be known. Through the statement $[\text{Eigenvec}, \text{Eigenvalue}] = \text{eig}(Ac)$, where $\text{eig}(Ac)$ is a MATLAB subroutine, it is possible to identify the (i,i) and (j,j) eigenvalues of the pitching and heaving modes and the corresponding i^{th} , j^{th} columns of the 14×14 matrix of eigenvectors.

In the example studied, the eigenvalue $3.11e-004+4.44e+001i$ corresponding to zero damping ratio is the $(7,7)$ term of the diagonal matrix of the eigenvalues. Hence, the amplitude ratio is obtained as the ratio of the eigenvectors moduli of the 5th (h/B) and 6th (α) rows, belonging to the column 7 of the matrix of the eigenvectors :

$$|h_0 e^{i\omega t}| / |\alpha_0 e^{i(\omega t + \varphi)}| = \sqrt{\frac{(-1.8943 e-003)^2 + [(4.9899 e-003)i]^2}{(-4.6135 e-005)^2 + [(5.4820 e-003)i]^2}} = \frac{5.3374 e-003}{5.4822 e-003} = 0.97358$$

Likewise, the phase difference φ can be calculated from the 6th and 5th rows of column 7 of the eigenvectors as:

$$\varphi = \tan^{-1}(5.482e-03 / -4.6135e-05) - \tan^{-1}(4.9899e-03 / -1.8943e-03) = 19.29^\circ.$$

6.6.2. Impulse responses

The impulse responses are obtained with the MATLAB subroutine "lsim", which simulates LTI (linear, time-invariant) model responses to arbitrary inputs. When invoked with left-hand arguments, $[y,t,x] = \text{lsim}(\text{sys},u,t,x_0)$ refers to state-space models with initial state x_0 . It returns the output response y , the time vector t used for simulation, and the state trajectories x , which signify in the present case the amplitudes of velocities and displacements, represented by the vector

$$\left[\frac{\dot{h}}{B} \quad \dot{\alpha} \quad \delta_1 \quad \delta_2 \quad \frac{h}{B} \quad \alpha \quad \delta_1 \quad \delta_2 \right]'$$

In the present case, the subroutine "lsim" was called by the statement $[Yres_c, x_res_c] = \text{lsim}(Ac, B, C, D, Uext, T, X0)$, where "sys" is the state space

model constituted by matrices A_c , B , C , D ($D=0$), $u = U_{ext}$, $t = T$ and $x_0 = X_0$. The important fact here is that the matrix A_c is the Laplace transformed state matrix assembled for a certain wind velocity.

The initial state is represented by a velocity impulse $\frac{d\alpha}{dt} = \frac{1}{I_\alpha}$ in the center of the deck : $x_0 = \left[0 \quad \frac{1}{I_\alpha} \quad 0 \right]$.

Vector T in $l_{sim}(A_c, B, C, D, U_{ext}, T, X_0)$ varies from 0 to 1 second in intervals of 0,001 seconds.

Graphs of the amplitudes of h/B and α of the uncontrolled system and $\left[\frac{h}{B} \quad \alpha \quad \delta_1 \quad \delta_2 \quad \dot{\frac{h}{B}} \quad \dot{\alpha} \quad \dot{\delta}_1 \quad \dot{\delta}_2 \right]'$ of the controlled system are shown in the next sections.

6.7. Results of the closed loop system for $U_g = 9 \text{ m/s}$, $\rho_q = 1$, $\rho_r = 5$.

6.7.1. Numerical data

The state matrix corresponding to the critical velocity of 11.910 m/s is presented in Table 6-1.

-4.8291	-2.7269	-0.0188	-0.0188	-158.2000	-205.6000	-20.7960	-20.7960	-161.0200	-151.6400	-31.3620	-9.9548	-31.3620	-9.9548
7.9097	-3.8757	0.0759	-0.0831	139.2200	-351.2600	92.3540	-83.5590	334.7600	339.2500	139.2700	44.2080	-126.0100	-39.9980
132.3200	-134.9000	-52.7790	0.0000	536.4300	-597.2800	-2076.4000	355.7200	0.0000	0.0000	0.0000	0.0000	0.0000	0.0000
-27.3550	64.1910	0.0000	-52.8670	-163.0400	-268.5900	317.2400	-1647.9000	0.0000	0.0000	0.0000	0.0000	0.0000	0.0000
1.0000	0.0000	0.0000	0.0000	0.0000	0.0000	0.0000	0.0000	0.0000	0.0000	0.0000	0.0000	0.0000	0.0000
0.0000	1.0000	0.0000	0.0000	0.0000	0.0000	0.0000	0.0000	0.0000	0.0000	0.0000	0.0000	0.0000	0.0000
0.0000	0.0000	1.0000	0.0000	0.0000	0.0000	0.0000	0.0000	0.0000	0.0000	0.0000	0.0000	0.0000	0.0000
0.0000	0.0000	0.0000	1.0000	0.0000	0.0000	0.0000	0.0000	0.0000	0.0000	0.0000	0.0000	0.0000	0.0000
0.0000	0.0000	0.0000	0.0000	-0.5887	3.1809	0.0000	0.0000	-7.7795	0.0000	0.0000	0.0000	0.0000	0.0000
0.0000	0.0000	0.0000	0.0000	-9.3767	10.5610	0.0000	0.0000	0.0000	-30.4250	0.0000	0.0000	0.0000	0.0000
0.0000	0.0000	0.0000	0.0000	-0.1158	0.5448	0.4869	0.0000	0.0000	0.0000	-13.7310	0.0000	0.0000	0.0000
0.0000	0.0000	0.0000	0.0000	-142.0900	128.9600	57.9110	0.0000	0.0000	0.0000	0.0000	-80.8460	0.0000	0.0000
0.0000	0.0000	0.0000	0.0000	-0.1158	0.4290	0.0000	0.4869	0.0000	0.0000	0.0000	0.0000	-13.7310	0.0000
0.0000	0.0000	0.0000	0.0000	-142.0900	-13.1330	0.0000	57.9110	0.0000	0.0000	0.0000	0.0000	0.0000	-80.8460

Table 6-1- State Matrix $A_c = A - BKC$ for $U_{crit} = 11.910 \text{ m/s}$.

The results of the complex eigenvalue analysis are shown in Table 6-2.

	Eigenvalues	Damping	Frequency (rad/s)	Diagonal Matrix of the Eigenvalues	State Vector	Column 5 - Matrix of the Eigenvectors	Column 9 - Matrix of the Eigenvectors
α	$9.96e-003 + 1.78e+001i$	-0.00056	17.8	$\begin{matrix} \text{Term (9,9)} \\ -2.6941e+001 + 1.4357e+001i \\ \text{Term (5,5)} \\ 9.9582e-003 + 1.7777e+001i \end{matrix}$	$(dh/dt)/B$	-6.05E-01	-5.0166e-002 -5.5829e-002i
	$9.96e-003 - 1.78e+001i$	-0.00056	17.8		(da/dt)	$-5.0892e-001 + 3.2203e-001i$	$2.1965e-001 + 1.2026e-001i$
	-1.5	1	1.5		$(d\delta_1/dt)$	$1.8745e-001 - 3.6939e-001i$	8.52E-01
	-11.7	1	11.7		$(d\delta_2/dt)$	$-2.0962e-001 - 2.1969e-001i$	$-4.4252e-001 - 7.6205e-002i$
	-13.7	1	13.7		h/B	$-1.9079e-005 + 3.4058e-002i$	$5.9019e-004 + 2.3868e-003i$
	-14.9	1	14.9		α	$1.8099e-002 + 2.8639e-002i$	$-4.4970e-003 - 6.8605e-003i$
	$-1.79e+001 + 3.55e+001i$	0.45	39.8		δ_1	$-2.0774e-002 - 1.0556e-002i$	$-2.4633e-002 - 1.3127e-002i$
	$-1.79e+001 - 3.55e+001i$	0.45	39.8		δ_2	$-1.2365e-002 + 1.1785e-002i$	$1.1619e-002 + 9.0204e-003i$
	$-2.58e+001 + 2.70e+001i$	0.691	37.4		x_1	$4.5438e-003 - 1.2483e-003i$	$-9.1972e-005 + 1.1433e-003i$
	$-2.58e+001 - 2.70e+001i$	0.691	37.4		x_2	$4.4457e-003 - 3.1516e-003i$	$-7.0848e-003 + 1.9741e-003i$
h/B	$-2.69e+001 + 1.44e+001i$	0.883	30.5		X_{w11}	$2.2272e-004 + 1.8635e-004i$	$1.1118e-004 + 9.0859e-004i$
	$-2.69e+001 - 1.44e+001i$	0.883	30.5		X_{w12}	$8.8167e-003 - 2.3673e-002i$	$-4.5362e-002 - 2.4725e-002i$
	-78.1	1	78.1		X_{w21}	$5.4344e-004 + 3.2182e-004i$	$-8.2794e-005 - 1.7874e-004i$
	-80.4	1	80.4		X_{w22}	$-2.2977e-002 - 5.1009e-002i$	$1.2487e-002 + 1.7451e-003i$

Table 6-2- Eigenvalues, damping ratios, frequencies and eigenvectors of interest obtained from the complex eigenvalue analysis of the state matrix A_c .

The amplitude ratio is

$$|h_0 e^{i\omega t}| / |\alpha_0 e^{i(\omega t + \varphi)}| = \sqrt{\frac{(1.9079 e-005)^2 + [(3.4058 e-002)i]^2}{(1.8099 e-002)^2 + [(2.8639 e-002)i]^2}} = 1.0053$$

The phase difference φ is

$$\varphi = \tan^{-1}(0.028639/0.018099) - \tan^{-1}(0.034058/-0.019079e-003) = 147.6762^\circ.$$

Plots of frequencies and damping ratios versus wind velocities follow. Curves representing frequencies other than heaving and pitching modes are without practical importance.

6.7.2. Plots of frequencies and damping ratios for $U = 9 \text{ m/s}$.

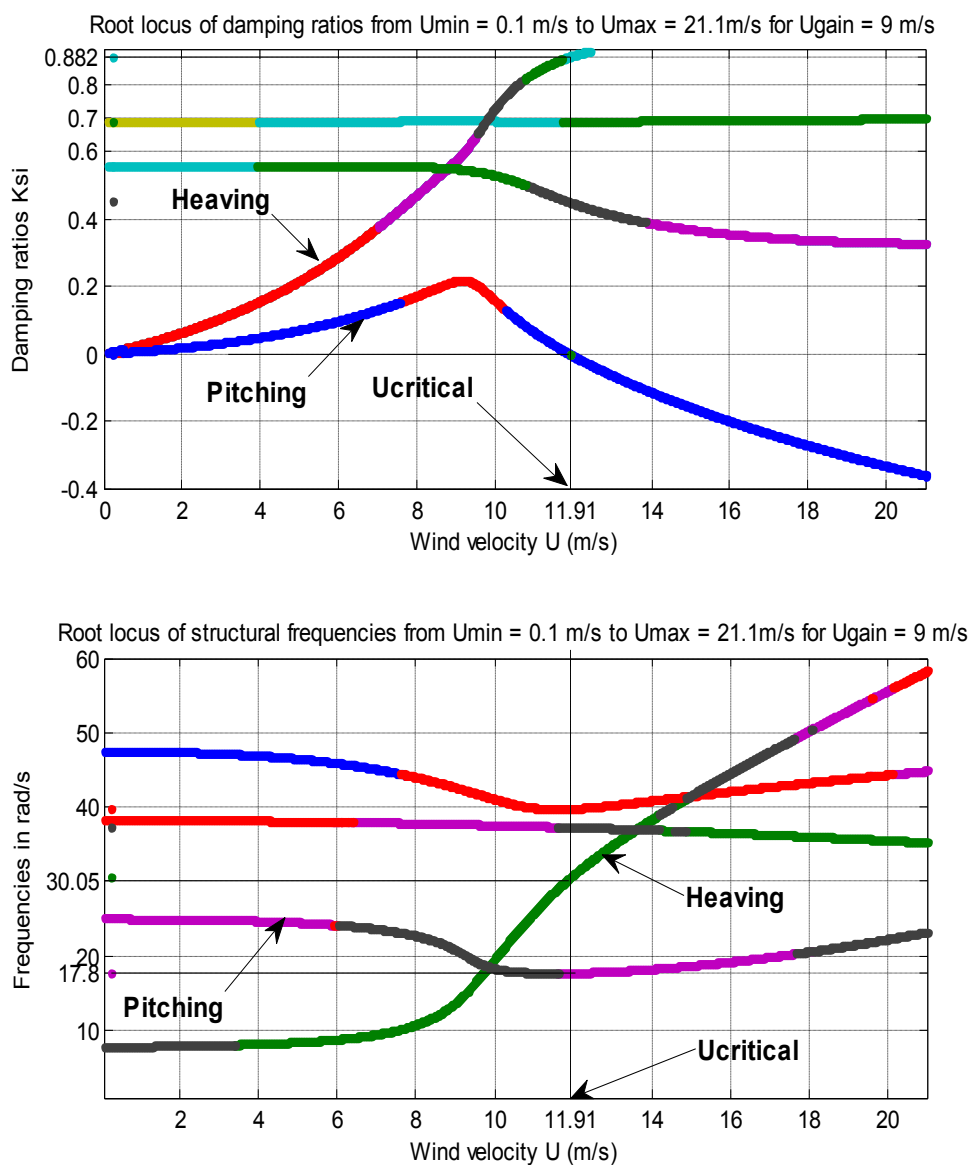


Figure 6-1 - Variations of damping ratios and frequencies of closed-loop system with gain design for $U_g = 9 \text{ m/s}$ versus wind speed.

The damping ratio of the pitching mode approaches zero as the wind speed approaches the critical speed, 11.91 m/s . Therefore, pitching still leads to the instability of the system, as in the uncontrolled system.

6.7.3. Impulse responses

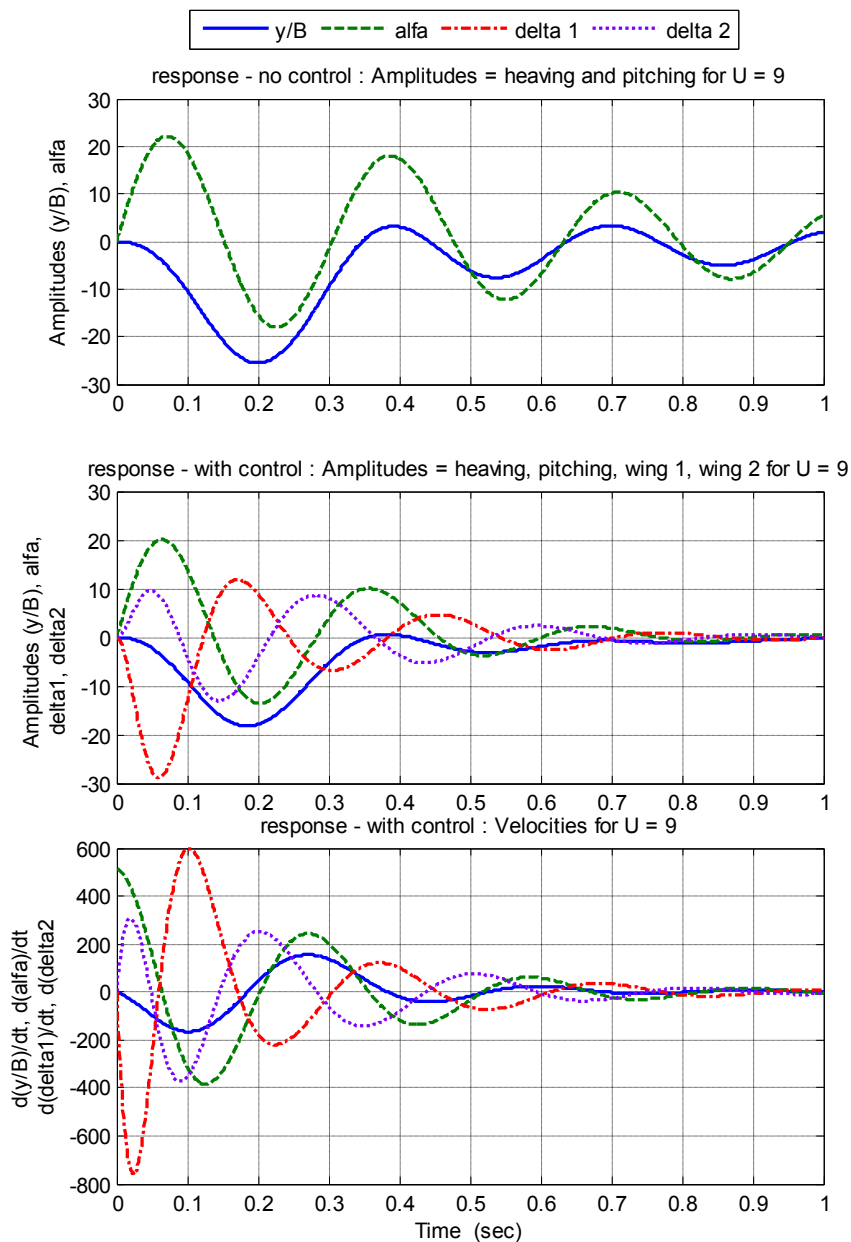


Figure 6-2 - Impulse response of closed loop system with gain calculated for $U_g = 9$ m/s at $U = 9$ m/s.

Note that the impulse input to the system was:

$$x_0 = \left[0 \quad \frac{1}{I_\alpha} \quad 0 \right] = [0 \ 516.93 \ 0 \ 0 \ 0 \ 0 \ 0 \ 0 \ 0 \ 0 \ 0 \ 0 \ 0 \ 0 \ 0 \ 0 \ 0 \ 0 \ 0 \ 0]$$

The responses to these initial conditions ($t=0$) in the controlled system are shown in Figure 6-2. The stability of the system is assured for $U_g = 9$ m/s. at $U = 9$ m/s.

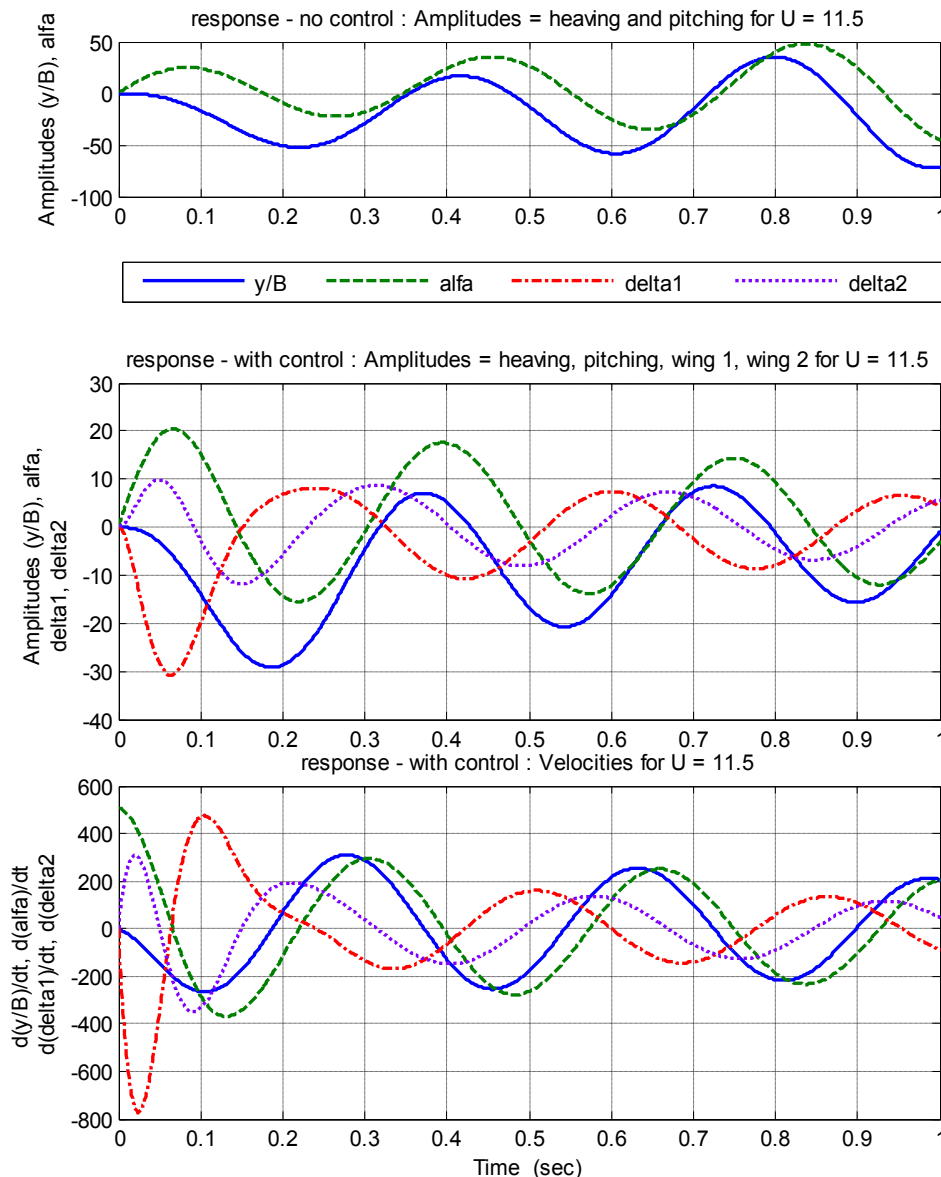


Figure 6-3 - Impulse response of closed-loop system with gain calculated for $U_g = 9$ m/s at $U = 11.7$ m/s (near the critical 11.91m/s)

Note that the impulse input to the system was:

$$x_0 = \left[0 \quad \frac{1}{I_\alpha} \quad 0 \right] = [0 \ 516.93 \ 0 \ 0 \ 0 \ 0 \ 0 \ 0 \ 0 \ 0 \ 0 \ 0 \ 0 \ 0 \ 0 \ 0]$$

The amplitude responses of the uncontrolled system tend to grow indefinitely. The amplitude responses in the two lower pictures of Figure 6-3 show the initial conditions for $t=0$ in the controlled system. The stability of the system for $U_d = 9$ m/s at $U = 9$ m/s is endangered as the wind velocity approaches the critical one, i.e., $U_{crit} = 11.91$ m/s.

6.8. Results of the closed loop system for $U_g = 11$ m/s, $\rho_q = 5$, $\rho_r = 30$.

6.8.1. Numerical data

The state matrix corresponding to the critical velocity of 12.7 m/s is presented in Table 6-3

The results of the complex eigenvalue analysis are shown in Table 6-4.

-5.1483	-2.9078	-0.020049	-0.020049	-171.38	-233.78	-23.647	-23.647	-183.09	-172.42	-35.66	-11.319	-3.57E+01	-1.13E+01
8.43E+00	-4.13E+00	8.10E-02	-8.86E-02	1.58E+02	-3.13E+02	1.05E+02	-9.50E+01	3.81E+02	3.86E+02	1.58E+02	5.03E+01	-1.43E+02	-4.55E+01
1.09E+02	-1.65E+02	-5.28E+01	0	8.19E+02	-1.08E+03	-2.23E+03	7.48E+00	0	0	0	0	0	0
-6.28E+01	1.24E+02	0	-5.29E+01	-5.43E+02	3.17E+02	6.32E+02	-1.60E+03	0	0	0	0	0	0
1.00E+00	0	0	0	0	0	0	0	0	0	0	0	0	0
0	1.00E+00	0	0	0	0	0	0	0	0	0	0	0	0
0	0	1.00E+00	0	0	0	0	0	0	0	0	0	0	0
0	0	0	1.00E+00	0	0	0	0	0	0	0	0	0	0
0	0	0	0	-6.28E-01	3.39E+00	0	0	-8.30E+00	0	0	0	0	0
0	0	0	0	-1.00E+01	1.13E+01	0	0	0	-3.24E+01	0	0	0	0
0	0	0	0	-1.23E-01	5.81E-01	5.19E-01	0	0	0	-1.46E+01	0	0	0
0	0	0	0	-1.52E+02	1.38E+02	6.18E+01	0	0	0	0	-8.62E+01	0	0
0	0	0	0	-1.23E-01	4.57E-01	0	5.19E-01	0	0	0	0	-1.46E+01	0
0	0	0	0	-1.52E+02	-1.40E+01	0	6.18E+01	0	0	0	0	0	-8.62E+01

Table 6-3 - State Matrix $A_c = A - BKC$ for $U_{crit}=12.7$ m/s.

	Eigenvalues	Damping	Frequency (rad/s)	Diagonal Matrix of the Eigenvalues	State Vector	Column 5 - Matrix of the Eigenvectors	Column 9 - Matrix of the Eigenvectors
h/B	2.32e-003 + 1.77e+001i	-1.31E-04	1.77E+01		(dh/dt)/B	0.65385	-3.9398e-002 -2.1252e-002i
	2.32e-003 - 1.77e+001i	-1.31E-04	1.77E+01		(dα/dt)	4.8300e-001 +2.9407e-001i	1.8916e-001 +7.4729e-002i
	-2.57E+00	1.00E+00	2.57E+00		(dδ ₁ /dt)	-3.2158e-001 -2.4323e-001i	8.25E-01
	-1.23E+01	1.00E+00	1.23E+01		(dδ ₂ /dt)	2.6481e-001 -1.0980e-001i	-5.2236e-001 -2.6364e-002i
α	-1.25e+001 + 3.65e+001i	3.23E-01	3.86E+01	2.3214e-003 +1.7710e+001i	h/B	4.8394e-006 +3.6920e-002i	7.6907e-004 +1.0044e-003i
	-1.25e+001 - 3.65e+001i	3.23E-01	3.86E+01	Term (9,9)	α	-1.6601e-002 +2.7275e-002i	-4.0090e-003 -4.1185e-003i
	-14.6	1.00E+00	1.46E+01	-3.2273e+001 +1.4514e+001i	δ ₁	1.3732e-002 -1.8160e-002i	-2.1256e-002 -9.5597e-003i
	-15.6	1.00E+00	1.56E+01		δ ₂	6.2020e-003 +1.4952e-002i	1.3157e-002 +6.7342e-003i
	-2.71e+001 + 2.88e+001i	6.85E-01	3.96E+01		x1	-4.4320e-003 -1.1031e-003i	1.6003e-004 +7.0578e-004i
	-2.71e+001 - 2.88e+001i	6.85E-01	3.96E+01		x2	-3.6370e-003 -3.8959e-003i	-3.9296e-003 +3.5943e-003i
	-3.23e+001 + 1.45e+001i	9.12E-01	3.54E+01		x _{w11}	-1.3207e-004 -3.2811e-005i	2.4689e-004 +6.2750e-004i
	-3.23e+001 - 1.45e+001i	9.12E-01	3.54E+01		x _{w12}	-9.1989e-003 -3.6279e-002i	-4.0328e-002 -1.3414e-002i
	-8.27E+01	1.00E+00	8.27E+01		x _{w21}	-6.4728e-004 +2.8818e-004i	-1.2432e-004 -1.8676e-004i
	-8.58E+01	1.00E+00	8.58E+01		x _{w22}	1.8394e-002 -5.4828e-002i	1.4498e-002 +2.0566e-003i

Table 6-4- Eigenvalues, damping ratios, frequencies and eigenvectors of interest obtained from the complex eigenvalue analysis of the state matrix A_c .

The amplitude ratio is

$$|h_0 e^{i\omega t} / |\alpha_0 e^{i(\omega t + \varphi)}| = \sqrt{\frac{(4.84 e-006)^2 + [(3.692 e-002)i]^2}{(-1.66 e-002)^2 + [(2.7275 e-002)i]^2}} = 1.1563$$

The phase difference φ is

$$\varphi = \tan^{-1}(0.027275/-0.0166) - \tan^{-1}(0.03692/0.0484e-004) = -148.6656^\circ.$$

Plots of frequencies and damping ratios versus wind velocities follow. Curves representing frequencies other than heaving and pitching modes are without practical importance.

6.8.2. Plots of frequencies and damping factors for $U_g = 11$ m/s.

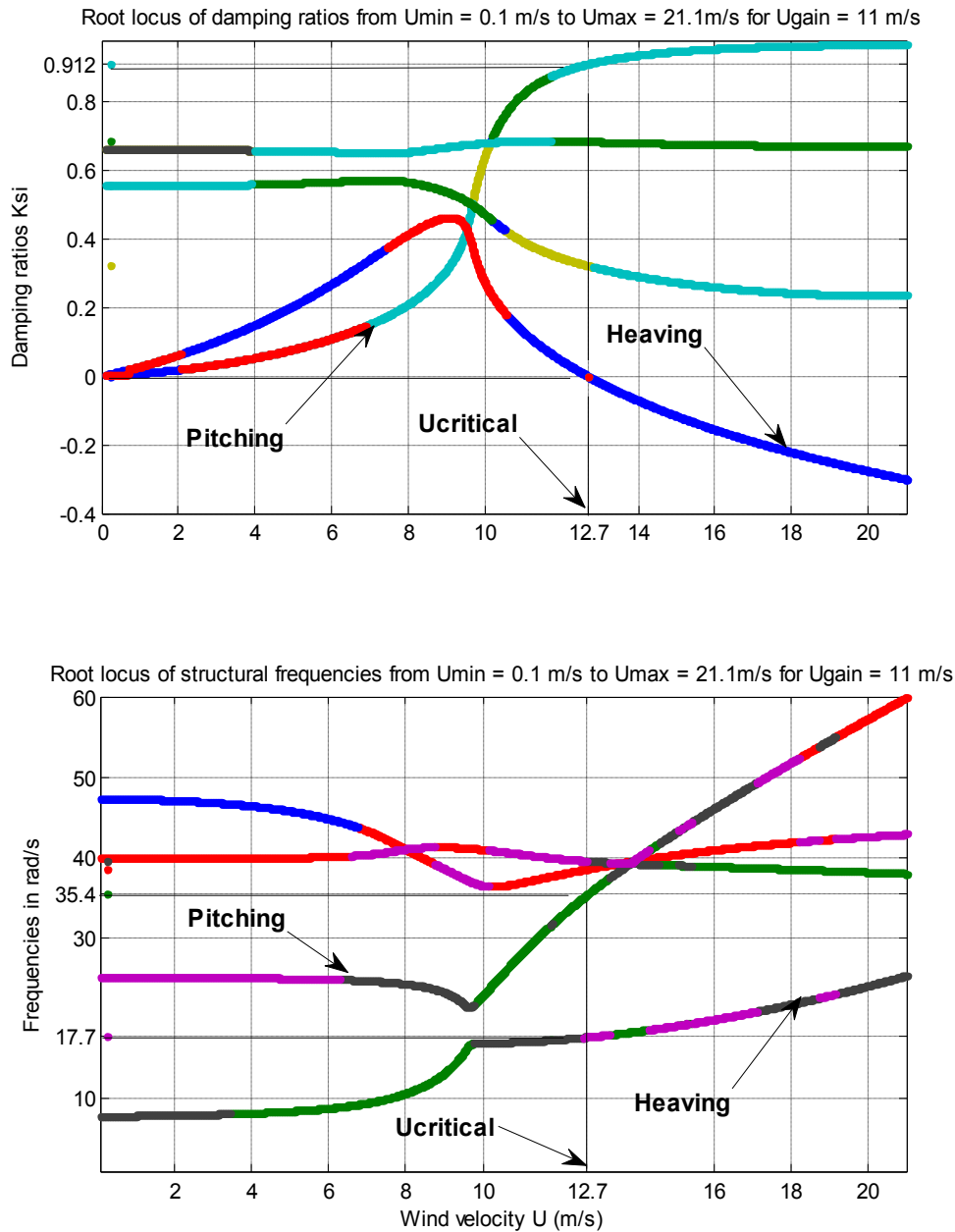


Figure 6-4 -Variations of damping ratios and structural frequencies of the closed-loop system with gain design for $U_g = 11$ m/s versus wind speed.

Note that the damping of the heaving mode approaches zero as the wind speed approaches the critical speed, 12.7 m/s. The plot shows that the pitching mode is controlled, and heaving is the critical mode, differently from the previous case, cp. Figure 6-1.

6.8.3. Impulse responses of the system for $U_g = 11 \text{ m/s}$.

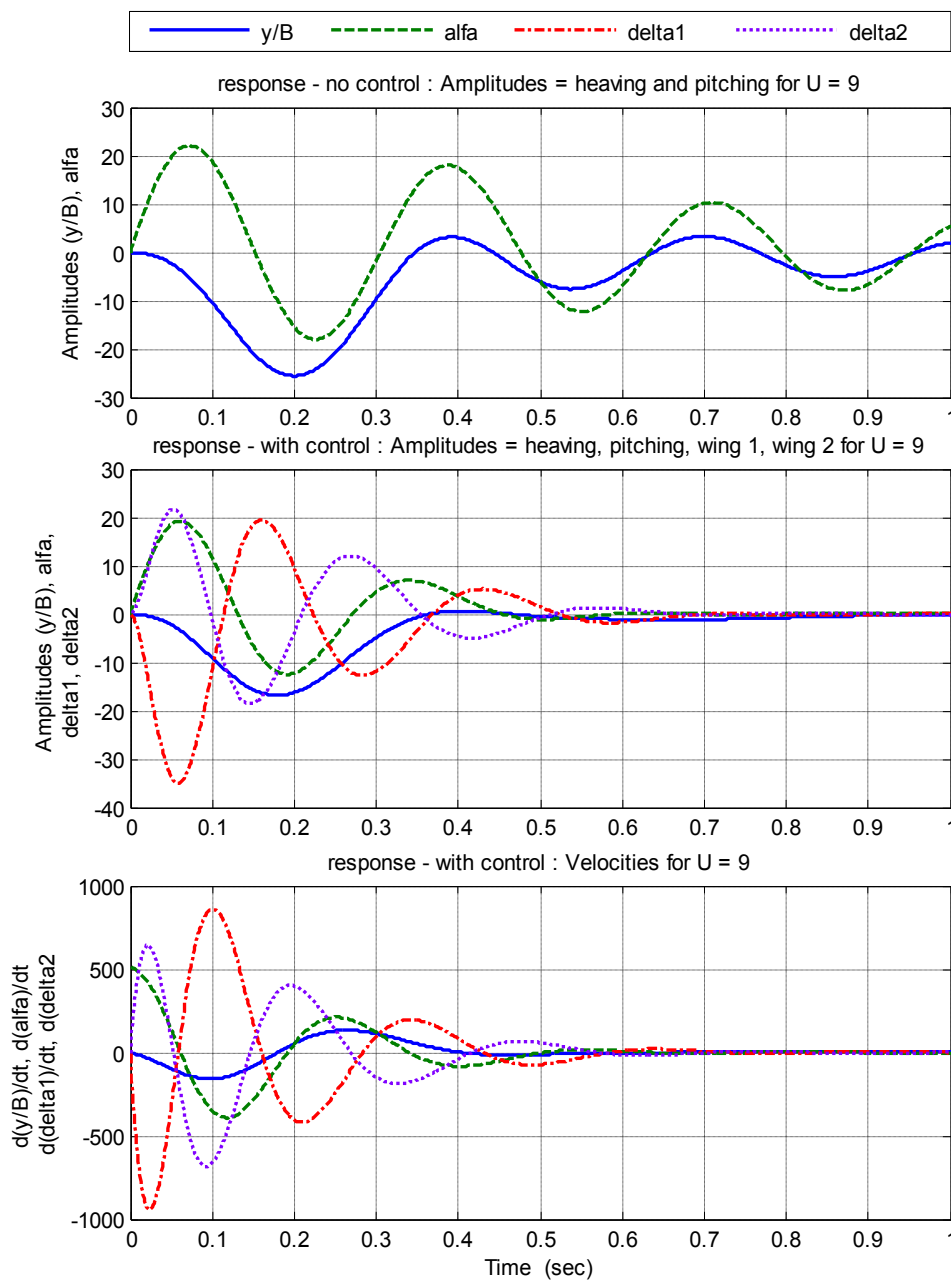


Figure 6-5 - Impulse response of closed-loop system with gain calculated for $U_g = 11 \text{ m/s}$ at $U = 9 \text{ m/s}$.

Note that the impulse input to the system was:

$$x_0 = \left[0 \quad \frac{1}{I_{\alpha}} \quad 0 \right] = [0 \quad 516.93 \quad 0 \quad 0]$$

The responses in the two lower figures shows these initial conditions ($t=0$) in the controlled system. The stability of the system is assured for $U_d = 11 \text{ m/s}$ at $U = 9 \text{ m/s}$.

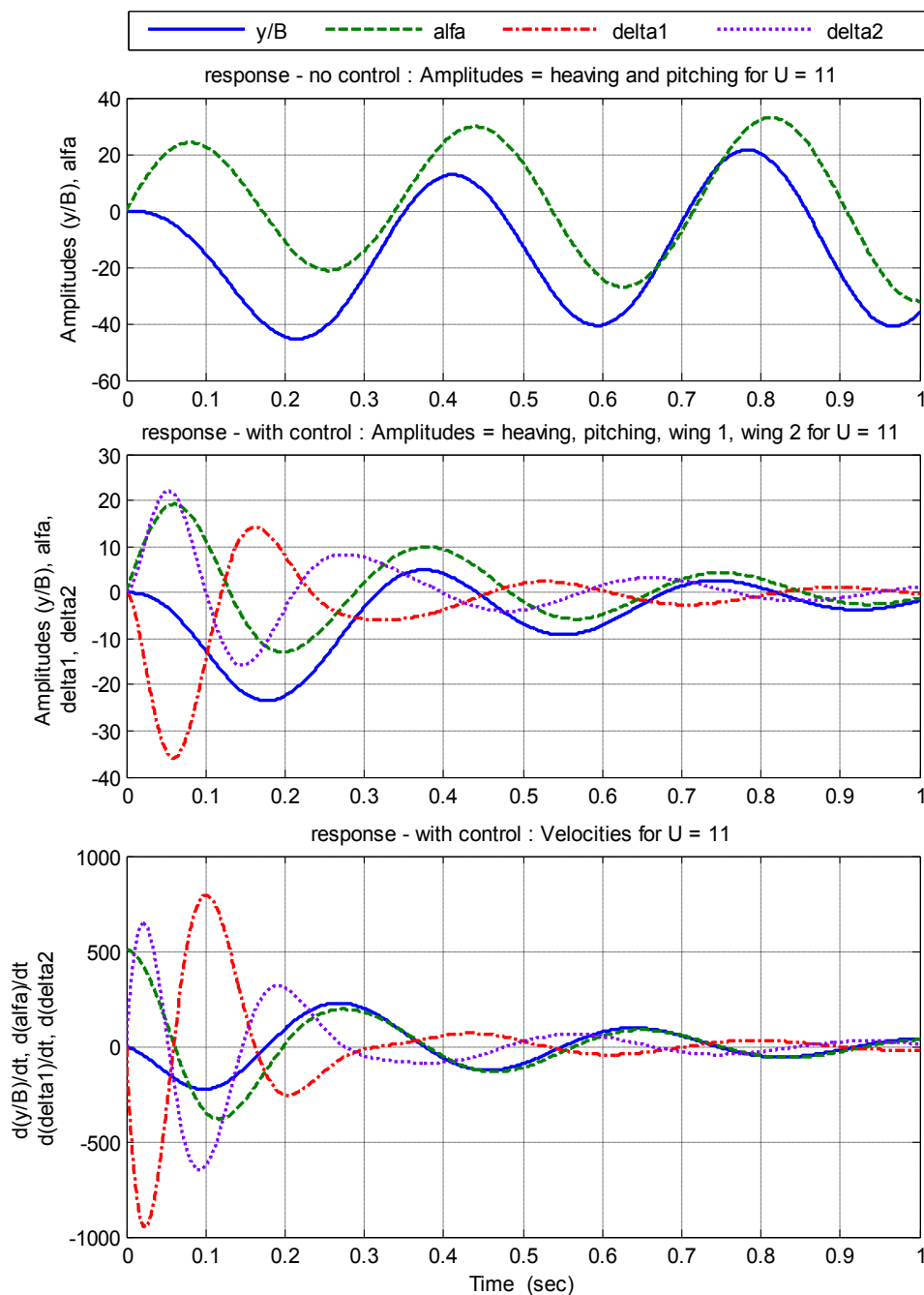


Figure 6-6 - Impulse response of the closed loop system with gain calculated for $U_g = 11$ m/s at $U=11.5$ m/s.

Note that the impulse input to the system was:

$$x_0 = \left[0 \quad \frac{1}{I_\alpha} \quad 0 \right] = [0 \ 516.93 \ 0 \ 0 \ 0 \ 0 \ 0 \ 0 \ 0 \ 0 \ 0 \ 0 \ 0 \ 0 \ 0]$$

The responses in the two lower pictures of Figure 6-6 show these initial conditions ($t = 0$) in the controlled system. The stability of the system is still assured at $U = 11$ m/s, although it takes longer to reach stability, compared to the behavior at 9 m/s (cp. Figure 6-5 and Figure 6-6).

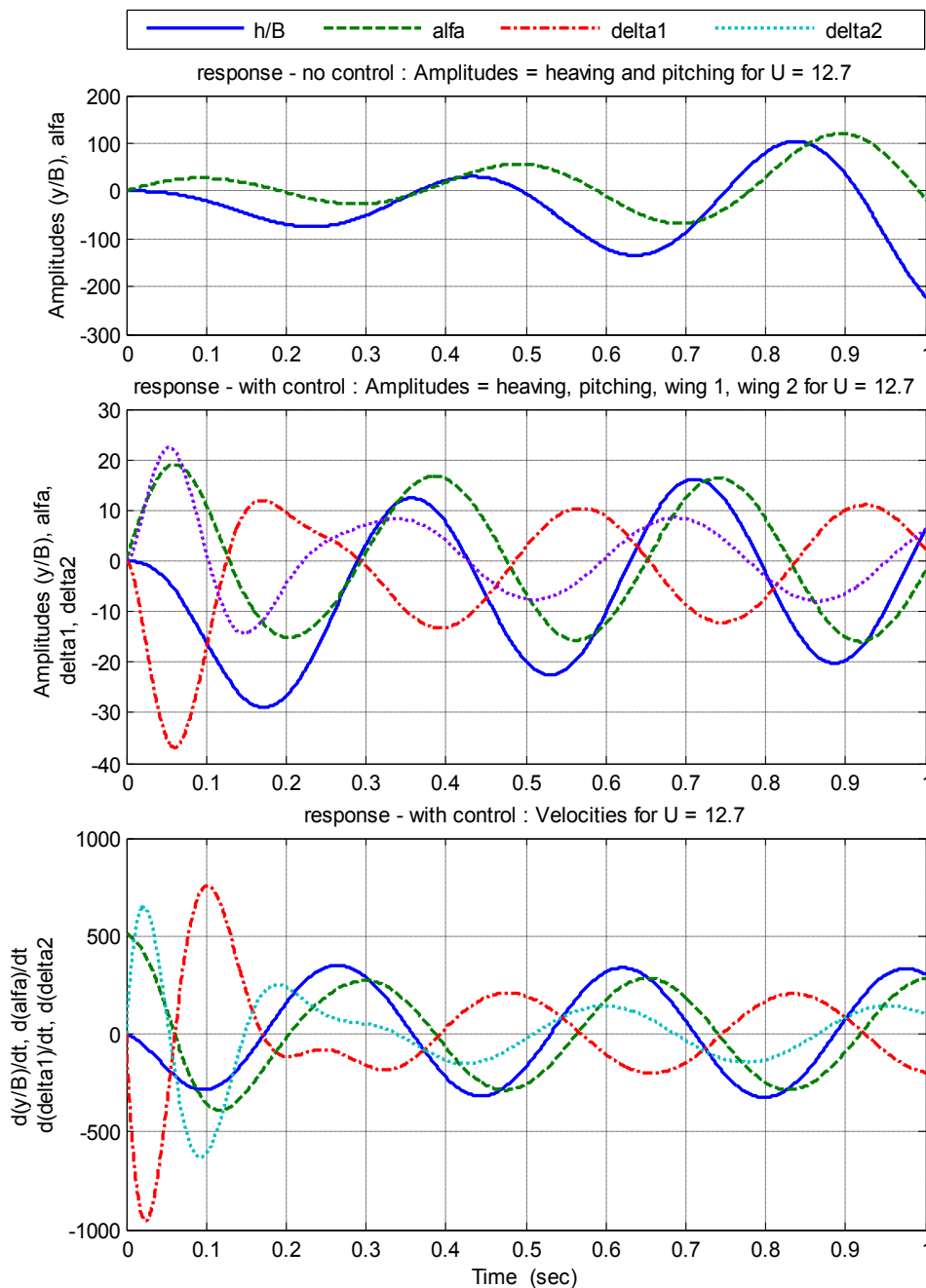


Figure 6-7 - Impulse response of closed-loop system with gain calculated for $U_g = 11$ m/s and $U = 12.7$ m/s.

The uncontrolled and the controlled systems are clearly unstable at 12.7 m/s.

6.9. Results of the closed loop system for $U_g = 15 \text{ m/s}$, $\rho_q = 10$, $\rho_r = 300$.

6.9.1. Numerical data

The state matrix corresponding to the critical velocity of 23.15 m/s is presented in Table 6-5.

The results of the complex eigenvalue analysis are shown in Table 6-6.

-9.37E+00	-5.30E+00	-3.65E-02	-3.65E-02	-4.25E+02	-7.77E+02	-7.86E+01	-7.86E+01	-6.08E+02	-5.73E+02	-1.18E+02	-3.76E+01	-1.18E+02	-3.76E+01
1.54E+01	-7.49E+00	1.48E-01	-1.62E-01	5.26E+02	4.17E+02	3.49E+02	-3.16E+02	1.26E+03	1.28E+03	5.26E+02	1.67E+02	-4.76E+02	-1.51E+02
1.69E+01	-2.00E+02	-5.28E+01	0	4.58E+02	-2.40E+03	-2.92E+03	6.02E+01	0	0	0	0	0	0
2.58E+01	1.15E+02	0	-5.29E+01	-3.15E+02	1.13E+03	5.10E+02	-1.35E+03	0	0	0	0	0	0
1.00E+00	0	0	0	0	0	0	0	0	0	0	0	0	0
0	1.00E+00	0	0	0	0	0	0	0	0	0	0	0	0
0	0	1.00E+00	0	0	0	0	0	0	0	0	0	0	0
0	0	0	1.00E+00	0	0	0	0	0	0	0	0	0	0
0	0	0	0	-1.14E+00	6.18E+00	0	0	-1.51E+01	0	0	0	0	0
0	0	0	0	-1.82E+01	2.05E+01	0	0	0	-5.91E+01	0	0	0	0
0	0	0	0	-2.25E-01	1.06E+00	9.46E-01	0	0	0	-2.67E+01	0	0	0
0	0	0	0	-2.76E+02	2.51E+02	1.13E+02	0	0	0	0	-1.57E+02	0	0
0	0	0	0	-2.25E-01	8.34E-01	0	9.46E-01	0	0	0	0	-2.67E+01	0
0	0	0	0	-2.76E+02	-2.55E+01	0	1.13E+02	0	0	0	0	0	-1.57E+02

Table 6-5 - State Matrix $A_c = A - BKC$ for $U_{crit} = 23.15 \text{ m/s}$.

	Eigenvalues	Damping	Frequency (rad/s)	Diagonal Matrix of the Eigenvalues	State Vector	Column 9 - Matrix of the Eigenvectors	Column 7 - Matrix of the Eigenvectors	
h/B	$1.19e-005 + 1.36e+001i$	-8.71E-07	1.36E+01		(dh/dt)/B	9.16E-01	-7.2761e-002 -2.0558e-002i	
	$1.19e-005 - 1.36e+001i$	-8.71E-07	1.36E+01		(da/dt)	$7.2613e-002 - 1.8528e-001i$	-1.8498e-001 -3.8266e-002i	
	$-5.56e+000 + 4.52e+001i$	1.22E-01	4.56E+01		(dδ ₁ /dt)	$-4.3801e-002 + 1.8288e-001i$	8.44E-01	
	$-5.56e+000 - 4.52e+001i$	1.22E-01	4.56E+01		Term (9,9)	(dδ ₂ /dt)	$1.6100e-001 + 1.7400e-001i$	-4.7035e-001 -1.5876e-001i
	$-1.65E+01$	1.00E+00	1.65E+01			h/B	$5.8471e-008 - 6.7129e-002i$	6.4272e-004 -1.5297e-003i
α	$-1.69e+001 + 2.65e+001i$	5.38E-01	3.15E+01	Term (7,7)	α	-1.3583e-002 -5.3233e-003i	1.3291e-003 -3.9265e-003i	
	$-1.69e+001 - 2.65e+001i$	5.38E-01	3.15E+01			δ ₁	$1.3407e-002 + 3.2111e-003i$	-2.2601e-003 +1.8373e-002i
	-1.96E+01	1.00E+00	1.96E+01			δ ₂	$1.2756e-002 - 1.1803e-002i$	4.7182e-003 -9.8192e-003i
	-2.45E+01	1.00E+00	2.45E+01			x1	$-1.6181e-003 + 4.3630e-003i$	5.1026e-004 +5.7603e-005i
	-2.74E+01	1.00E+00	2.74E+01			x2	$-3.5050e-004 + 1.8922e-002i$	6.5477e-004 -4.3137e-004i
	$-6.12e+001 + 1.70e+001i$	9.64E-01	6.35E+01			x _{w11}	$1.3956e-004 + 3.9731e-004i$	-2.5383e-004 +9.9191e-005i
	$-6.12e+001 - 1.70e+001i$	9.64E-01	6.35E+01			x _{w12}	$-2.3408e-003 + 1.1199e-001i$	-3.3212e-003 +8.9473e-003i
	-1.53E+02	1.00E+00	1.53E+02			x _{w21}	$1.4508e-005 - 2.6307e-005i$	2.6789e-004 -5.0921e-006i
	-1.56E+02	1.00E+00	1.56E+02			x _{w22}	$2.0770e-002 + 1.0859e-001i$	2.9894e-003 -2.9513e-003i

Table 6-6- Eigenvalues, damping ratios, frequencies and eigenvectors of interest obtained from the complex eigenvalue analysis of the state matrix A_c .

The amplitude ratio is

$$|h_0 e^{i\omega t}| / |\alpha_0 e^{i(\omega t + \varphi)}| = \frac{\sqrt{(5.85 \text{ e}^{-008})^2 + [(6.7129 \text{ e}^{-002})i]^2}}{\sqrt{(1.36 \text{ e}^{-002})^2 + [(5.3233 \text{ e}^{-003})i]^2}} = 4.6014$$

The phase difference φ is

$$\varphi = \tan^{-1}(0.0053233/0.0136) - \tan^{-1}(0.067129/0.0585e-006) = 111.4006^\circ.$$

Plots of frequencies and damping ratios versus wind velocities for $U_g = 15 \text{ m/s}$ follow. Curves representing frequencies other than heaving and pitching modes are without practical importance.

6.9.2. Numerical data

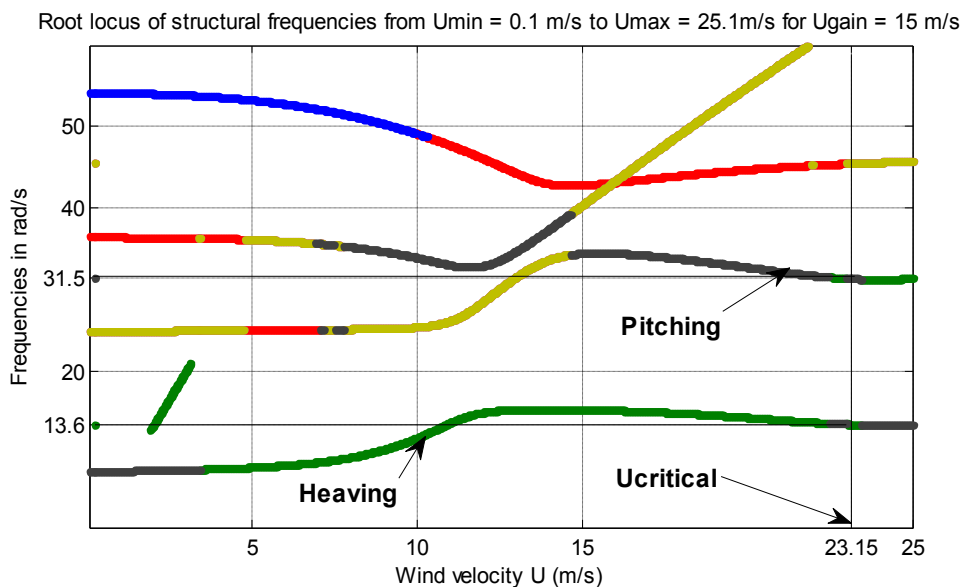
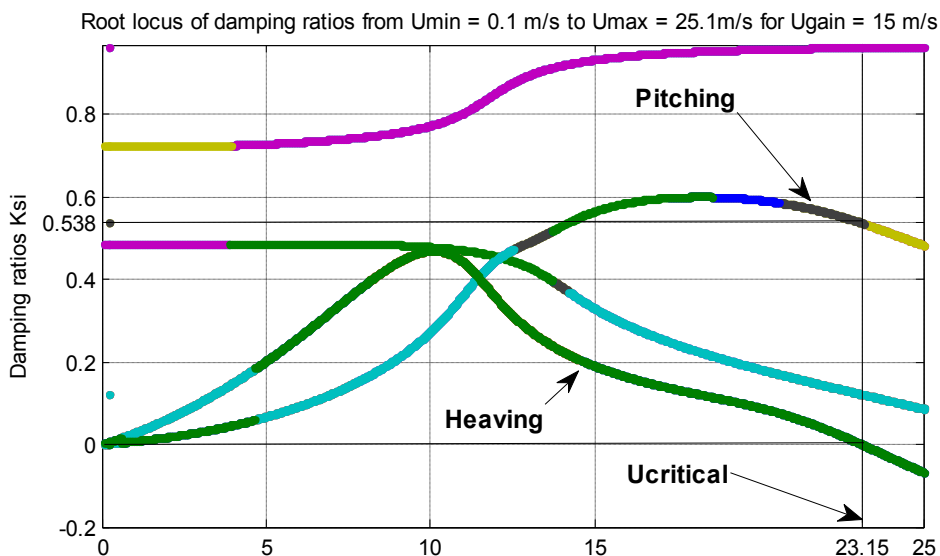


Figure 6-8 - Variations of modal frequency ω (rd/s) of closed-loop system with gain design for $U_g = 15$ m/s versus wind speed.

Note that the damping of the heaving mode approaches zero as the wind speed approaches the critical speed, 23.15 m/s. The plot shows that the pitching mode is controlled, and heaving is the critical mode, differently from the case shown in Figure 6-1.

6.9.3. Impulse responses

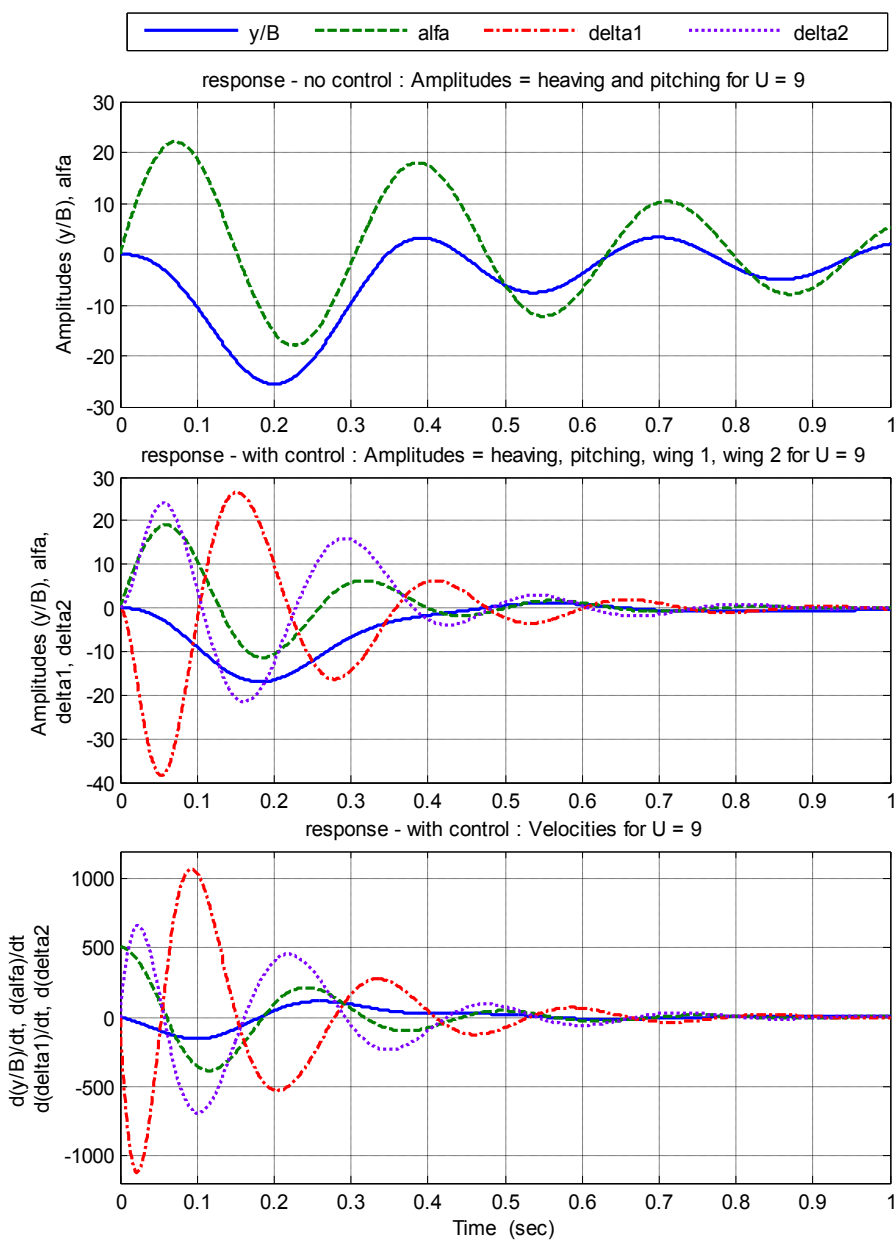


Figure 6-9 - Impulse response of closed loop system with gain calculated for $U_d=15\text{m/s}$ at 9 m/s .

The impulse input to the system was:

$$x_0 = \left[0 \quad \frac{1}{I_\alpha} \quad 0 \right] = [0 \ 516.93 \ 0 \ 0 \ 0 \ 0 \ 0 \ 0 \ 0 \ 0 \ 0 \ 0 \ 0]$$

The responses in the two lower pictures of Figure 6-9 show these initial conditions ($t=0$) in the controlled system. The stability of the system is assured for $U_g = 15\text{ m/s}$ at $U = 9\text{ m/s}$. The winglets rotate in opposite directions and must change amplitude signs in a very short time during the first second after the pulse.

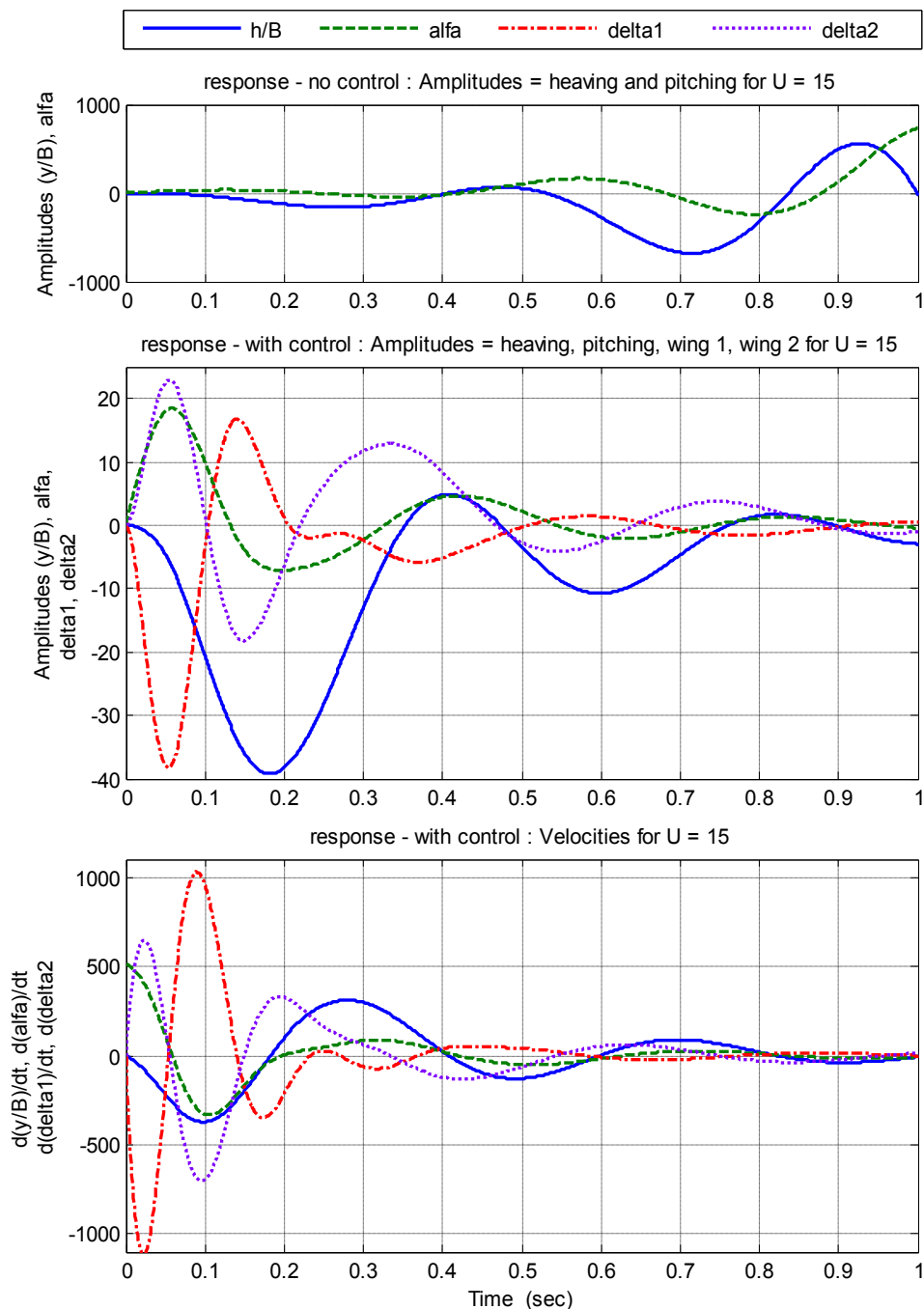


Figure 6-10 - Impulse response of closed loop system with gain calculated for $U_g=15\text{m/s}$ at 15 m/s

The impulse input to the system was:

$$x_0 = \left[0 \quad \frac{1}{I_\alpha} \quad 0 \right] = [0 \ 516.93 \ 0 \ 0 \ 0 \ 0 \ 0 \ 0 \ 0 \ 0 \ 0 \ 0 \ 0 \ 0 \ 0 \ 0 \ 0 \ 0 \ 0 \ 0 \ 0]$$

The responses in the two lower pictures of Figure 6-10 show these initial conditions ($t=0$) in the controlled system. The stability of the system is still assured at $U = 15 \text{ m/s}$, although it takes longer to reach stability. The heaving

amplitude doubles compared to the behavior of the system at 11 m/s. The winglets behave in the same manner as at 9 m/s (cp Figure 6-5 to Figure 6-6).

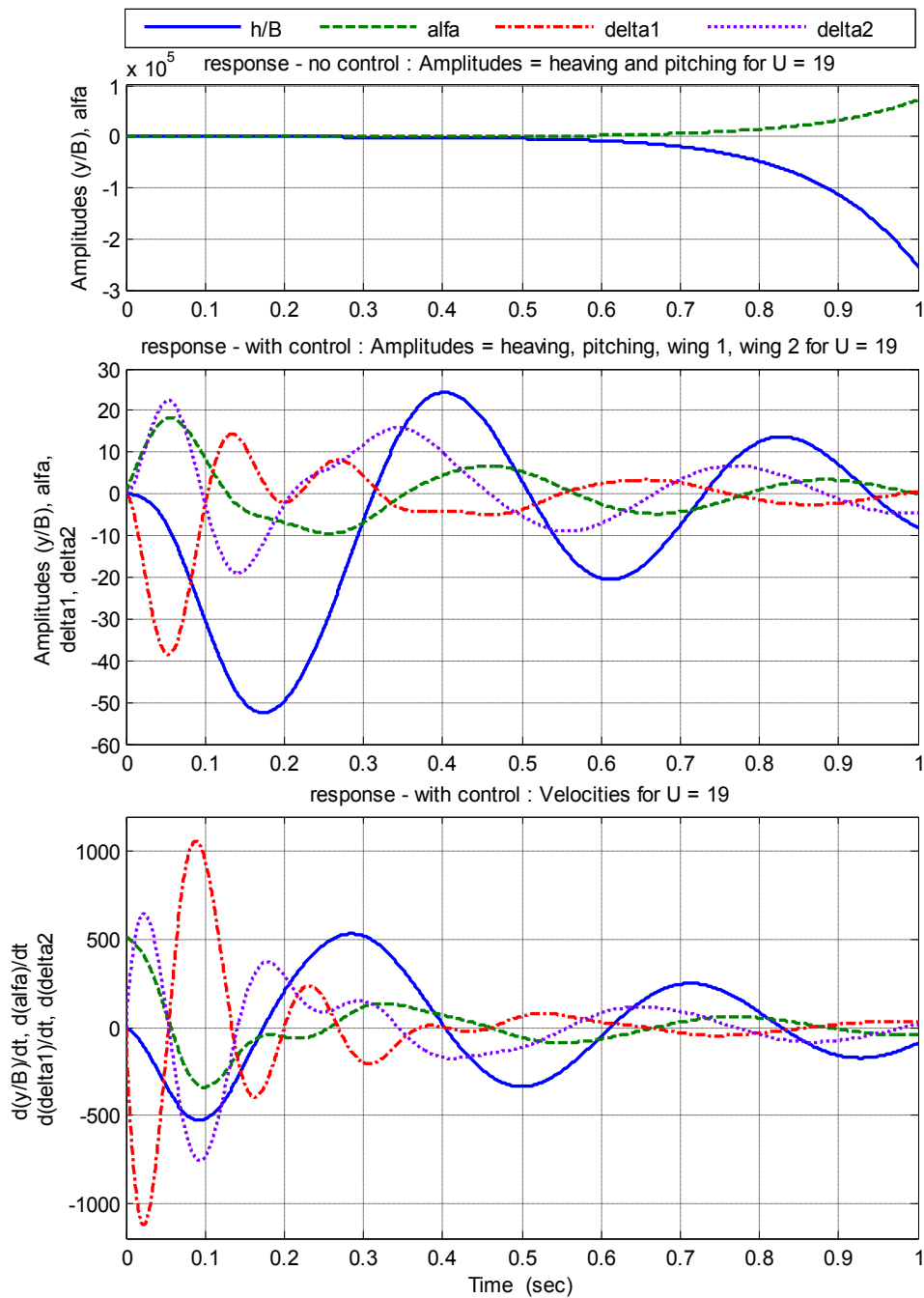


Figure 6-11 - Impulse response of closed loop system with gain calculated for $U_g=15\text{m/s}$ at 19 m/s

The stability of the system is still assured at $U = 19 \text{ m/s}$, although the amplitudes increase, compared to the system behavior at $U = 15 \text{ m/s}$. It also takes much longer to reach stability. The winglets behave in a similar manner as at 9, 11 and 15 m/s. (cp Figure 6-5 to Figure 6-6). The critical velocity is reached at $U = 23 \text{ m/s}$, according to (6.35).

6.10. Results of the closed loop system for $U_g = 19$ m/s, $\rho_q = 20$, $\rho_r = 500$.

6.10.1. Numerical data

The state matrix corresponding to the critical velocity of 30.67 m/s is presented in Table 6-7. The results of the complex eigenvalue analysis are shown in Table 6-8.

-12.409	-7.023	-0.048	-0.048	-699.590	-1363.600	-137.930	-137.930	-1067.900	-1005.700	-208.000	-66.022	-208.000	-66.022
20.370	-9.906	0.196	-0.214	923.350	1206.700	612.520	-554.180	2220.200	2250.000	923.670	293.200	-835.750	-265.270
88.555	-244.920	-52.779	0.000	549.870	-5288.400	-4760.000	-48.345	0.000	0.000	0.000	0.000	0.000	0.000
28.192	135.980	0.000	-52.867	-346.950	1925.000	864.110	-1589.500	0.000	0.000	0.000	0.000	0.000	0.000
1.000	0.000	0.000	0.000	0.000	0.000	0.000	0.000	0.000	0.000	0.000	0.000	0.000	0.000
0.000	1.000	0.000	0.000	0.000	0.000	0.000	0.000	0.000	0.000	0.000	0.000	0.000	0.000
0.000	0.000	1.000	0.000	0.000	0.000	0.000	0.000	0.000	0.000	0.000	0.000	0.000	0.000
0.000	0.000	0.000	1.000	0.000	0.000	0.000	0.000	0.000	0.000	0.000	0.000	0.000	0.000
0.000	0.000	0.000	0.000	-1.516	8.192	0.000	0.000	-20.035	0.000	0.000	0.000	0.000	0.000
0.000	0.000	0.000	0.000	-24.148	27.198	0.000	0.000	0.000	-78.354	0.000	0.000	0.000	0.000
0.000	0.000	0.000	0.000	-0.298	1.403	1.254	0.000	0.000	0.000	-35.362	0.000	0.000	0.000
0.000	0.000	0.000	0.000	-365.920	332.100	149.140	0.000	0.000	0.000	0.000	-208.200	0.000	0.000
0.000	0.000	0.000	0.000	-0.298	1.105	0.000	1.254	0.000	0.000	0.000	0.000	-35.362	0.000
0.000	0.000	0.000	0.000	-365.920	-33.822	0.000	149.140	0.000	0.000	0.000	0.000	0.000	-208.200

Table 6-7 - State Matrix for 30.67 m/s.

	Eigenvalues	Damping	Frequenc y (rad/s)	Diagonal Matrix of the Eigenvalues	State Vector	Column 7 - Matrix of the Eigenvectors	Column 9 - Matrix of the Eigenvectors
α	3.11e-004 + 4.44e+001i	-7.02E-06	4.44E+01		(dh/dt)/B	-2.2147e-001 -8.4076e-002i	0.88141
	3.11e-004 - 4.44e+001i	-7.02E-06	4.44E+01		(d α /dt)	-2.4332e-001 -2.0460e-003i	2.0646e-002 -1.3732e-001i
h/B	-7.66e-001 + 1.14e+001i	6.71E-02	1.14E+01		(d δ_1 /dt)	6.2371e-001 +9.9618e-002i	2.7290e-002 +3.2782e-001i
	-7.66e-001 - 1.14e+001i	6.71E-02	1.14E+01	Term (9,9)	(d δ_2 /dt)	-6.96E-01	5.5531e-002 +2.2228e-001i
	-7.59e+000 + 5.54e+001i	1.36E-01	5.59E+01	-7.6557e-001 +1.1385e+001i	h/B	-1.8943e-003 +4.9899e-003i	-5.1821e-003 -7.7067e-002i
	-7.59e+000 - 5.54e+001i	1.36E-01	5.59E+01	3.1138e-004 +4.4384e+001i	α	-4.6135e-005 +5.4820e-003i	-1.2128e-002 -9.9783e-004i
	-26.3	1.00E+00	2.63E+01	Term (7,7)	δ_1	2.2445e-003 -1.4053e-002i	2.8503e-002 -4.3135e-003i
	-3.25e+001 + 4.56e+000i	9.90E-01	3.28E+01		δ_2	-1.1009e-007 +1.5692e-002i	1.9109e-002 -6.1623e-003i
	-3.25e+001 - 4.56e+000i	9.90E-01	3.28E+01		x1	7.2001e-004 +2.6882e-004i	-1.0496e-003 +6.2597e-003i
	-36.2	1.00E+00	3.62E+01		x2	5.8642e-004 +3.2887e-005i	8.1235e-004 +2.3517e-002i
	-7.97e+001 + 2.38e+001i	9.58E-01	8.31E+01		x_{w11}	-1.2096e-004 -1.7105e-004i	6.6742e-004 +2.4769e-004i
	-7.97e+001 - 2.38e+001i	9.58E-01	8.31E+01		x_{w12}	2.5943e-003 -1.0645e-002i	1.7368e-002 +1.3030e-001i
	-203	1.00E+00	2.03E+02		x_{w21}	3.3981e-004 +2.5916e-004i	4.3718e-004 +2.6504e-004i
	-207	1.00E+00	2.07E+02		x_{w22}	3.5138e-003 +8.3094e-004i	3.1988e-002 +1.2992e-001i

Table 6-8 - Eigenvalues, damping ratios, frequencies and eigenvectors of interest.

The amplitude ratio is

$$|h_0 e^{i\omega t}| / |\alpha_0 e^{i(\omega t + \varphi)}| = \sqrt{\frac{(-1.8943 e-003)^2 + [(4.9899 e-003)i]^2}{(-4.6135 e-005)^2 + [(5.4820 e-003)i]^2}} \sim 1.$$

The phase difference φ is

$$\varphi = \tan^{-1}(5.4820e-003/-4.6135e-005) - \tan^{-1}(4.9899e-003/-1.8943e-003) \sim -2.0.$$

Plots of frequencies and damping ratios versus wind velocities follow. Curves representing frequencies other than heaving and pitching modes are without practical importance.

6.10.2. Plots of frequencies and damping factors for $U_g = 19$ m/s.

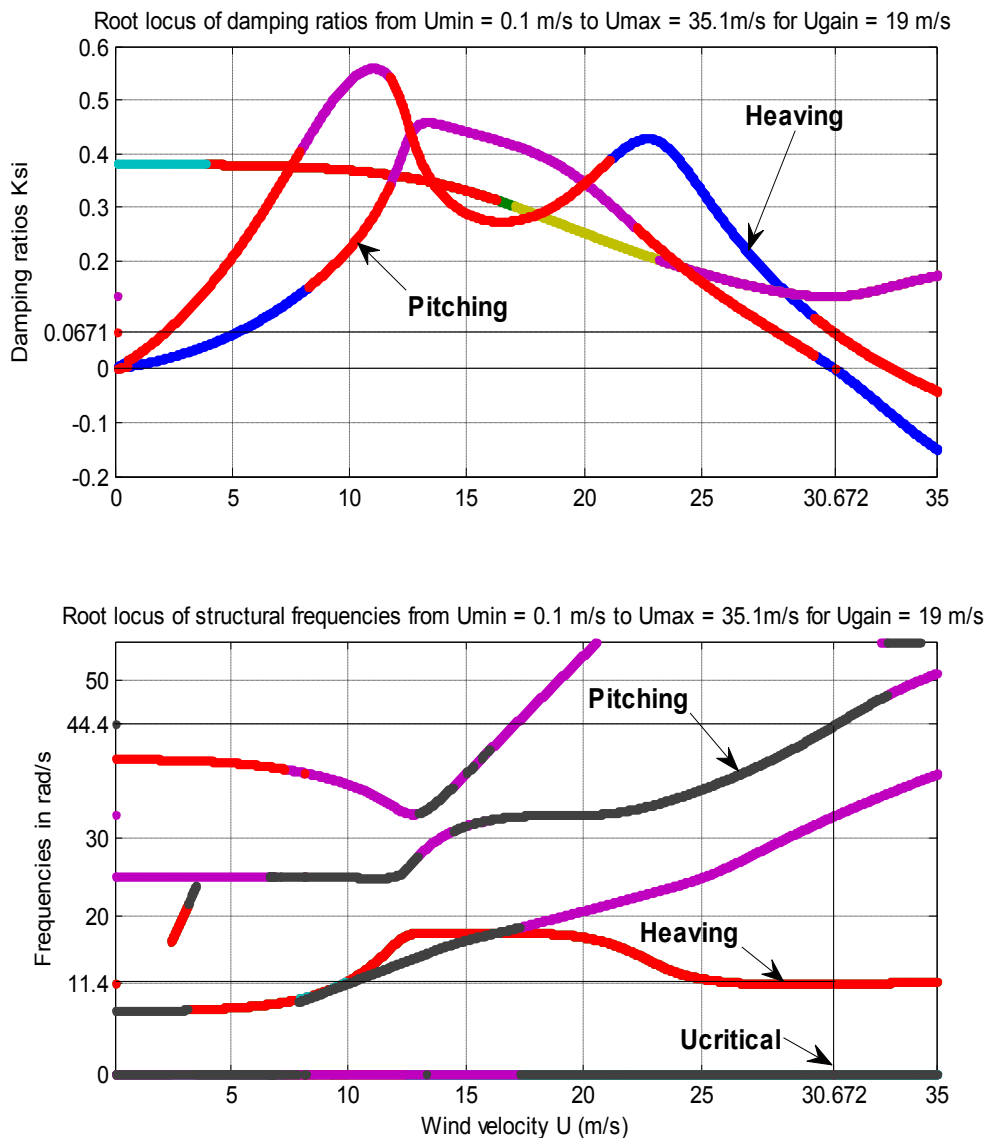


Figure 6-12 - Variations of modal frequency ω (rd/s) and damping ratios of closed-loop system with gain design for $U_g = 19$ m/s versus wind speed.

The damping of the pitching mode approaches zero as the wind speed approaches the critical speed, 30.672 m/s. The plot shows that the damping ratios of heaving and pitching are closer to each other than in the preceding case near the critical velocity. As the critical velocity is well beyond the limit of 21 m/s for which the performance of the controlled system is designed, the fact that pitching is again the unstable mode at 30.672 m/s is not important.

6.10.3. Impulse responses

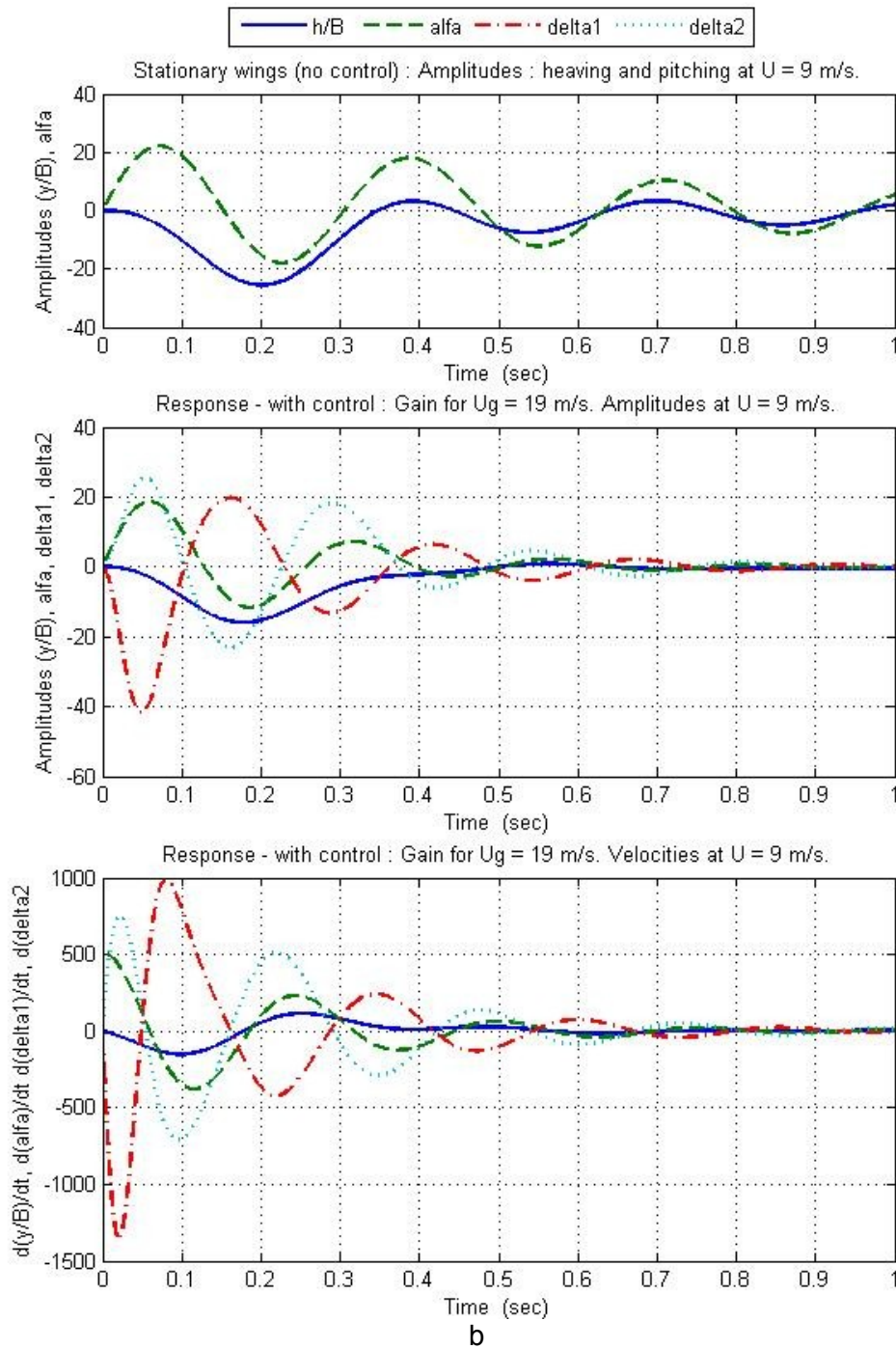


Figure 6-13 - Impulse response of closed loop system with gain calculated for $U_g=19$ m/s at 9 m/s

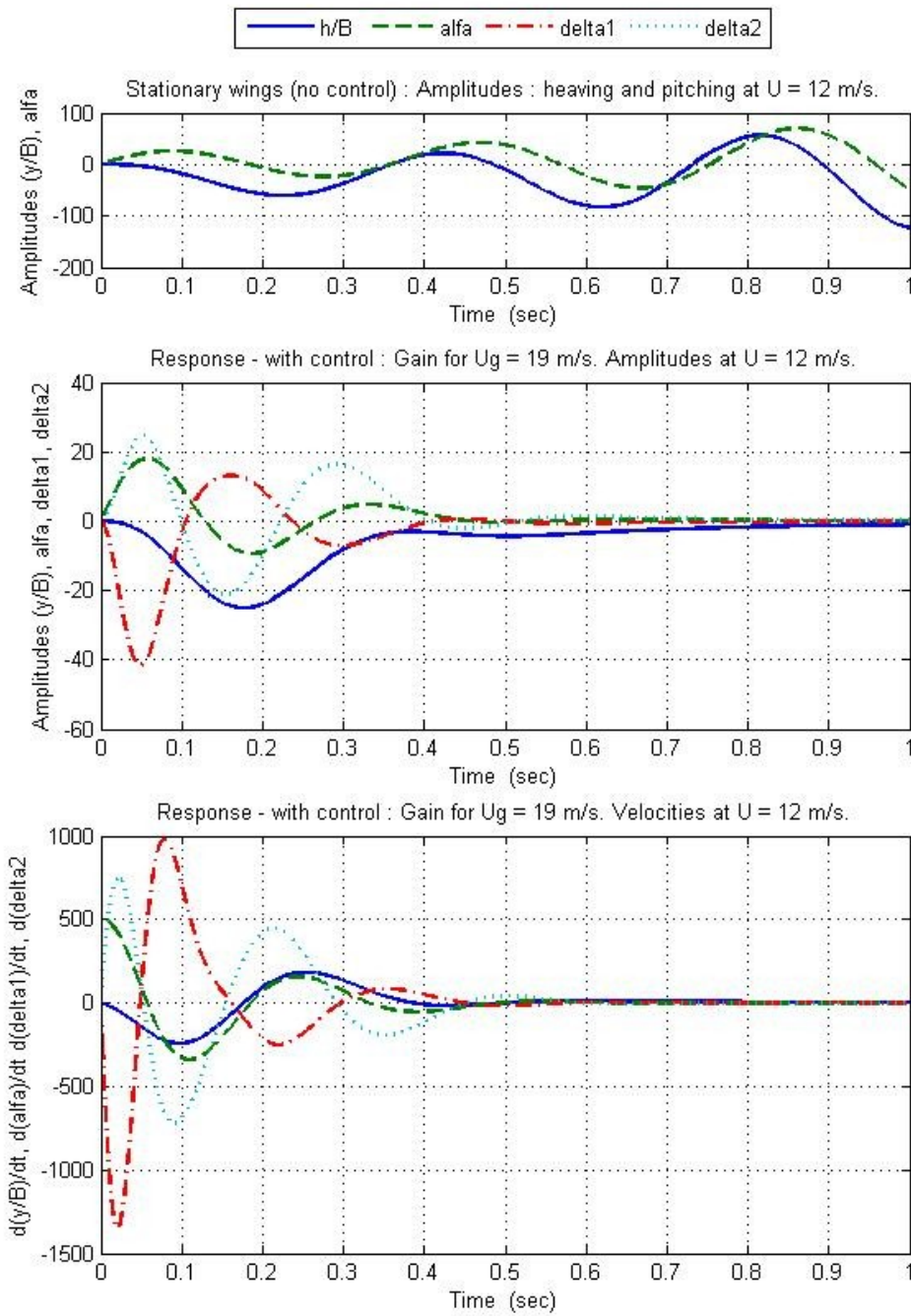


Figure 6-14 - Impulse response of closed loop system with gain calculated for $U_g=19$ m/s at 12 m/s.

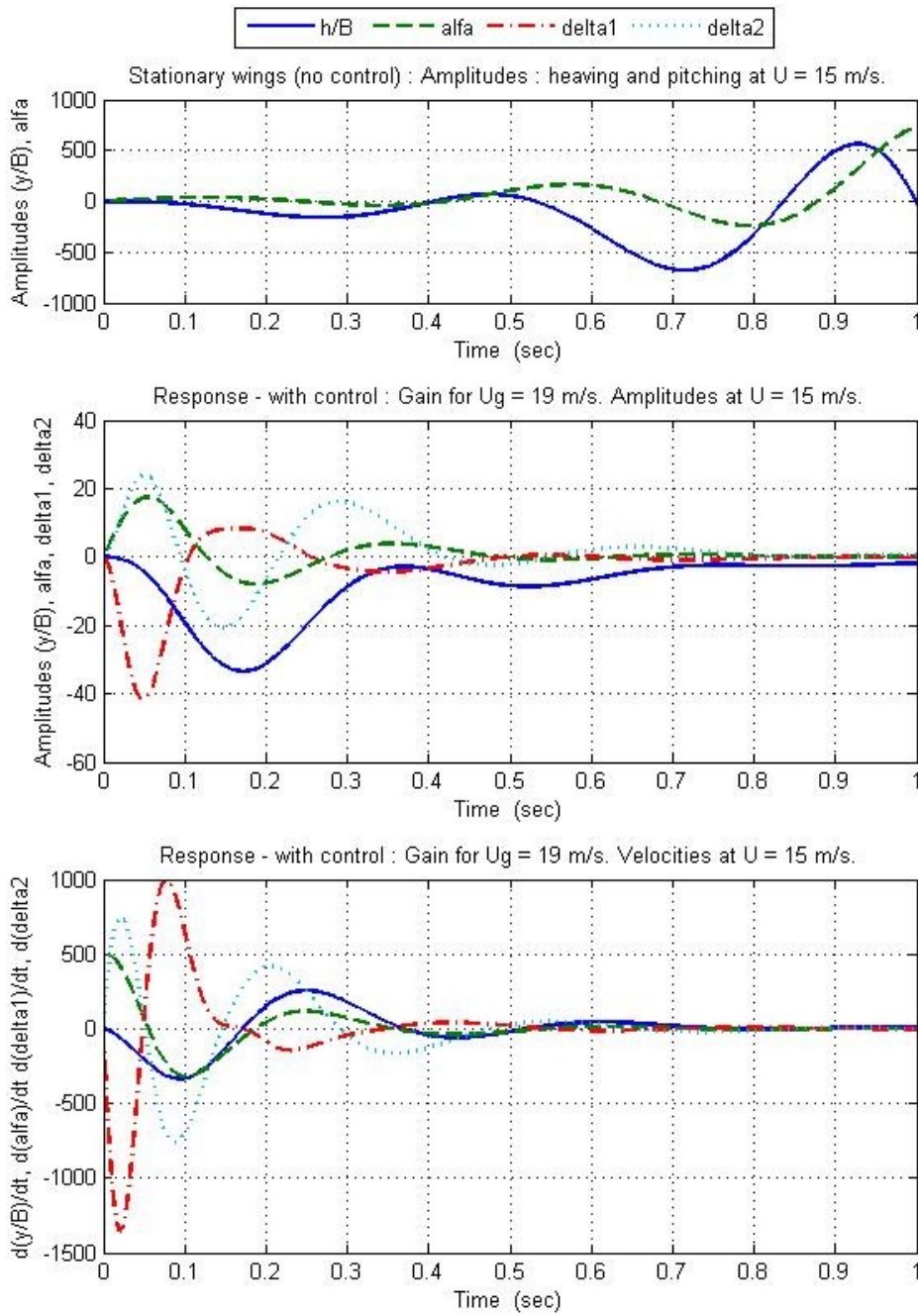


Figure 6-15 - Impulse response of closed loop system with gain calculated for $U_g=19$ m/s at 15 m/s.

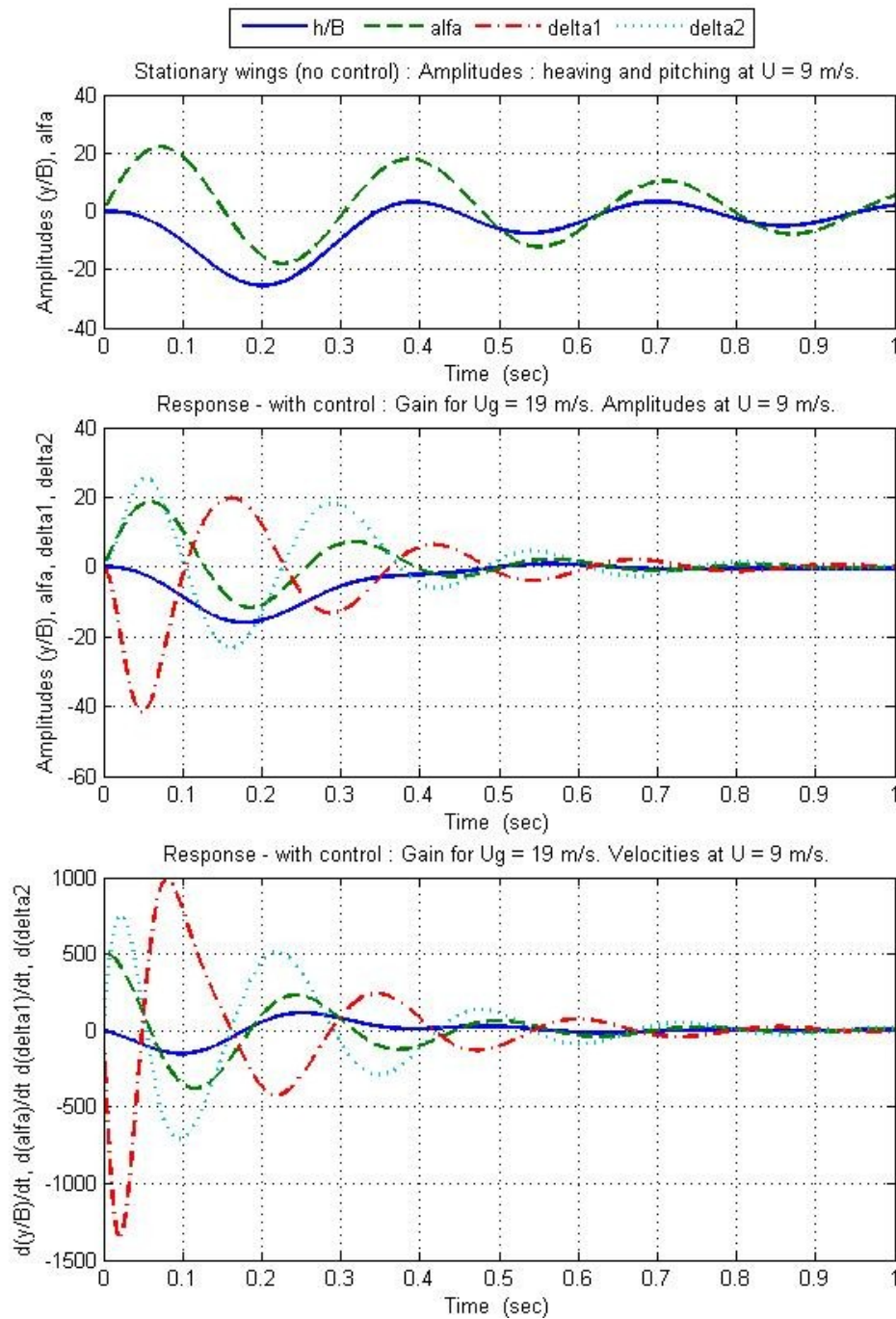


Figure 6-16 - Impulse response of closed loop system with gain calculated for $U_g=19$ m/s at 19 m/s

6.11. Conclusions

The optimal motion of the surfaces is governed by the pitching with some phase lead. Optimal control suggests that the most effective generation of the stabilizing aerodynamic forces is obtained when the leading surface rotates in the opposite direction and the trailing surface in the same direction as the deck. The

graphs also show that when the wind speed is lower than 11 m/s, the uncontrolled system is stable, and the amplitudes tend to zero in the first second after excitation. When the wind blows at 12.5 m/s the uncontrolled system is unstable when subjected to an initial impulse $d\alpha/dt = 1/I_\alpha$, as expected, since the gain was calculated for 11 m/s.

The main stabilizing action is due to the lift forces generated on the control surfaces which, multiplied by the arms e_1 and e_2 , result in large stabilizing moments. The simulations of various controllers show that some phase leading of the control surface rotation with respect to pitching is very important in the aerodynamic control. Control with gains that results in zero phase shift provides stability, but the wind speed at which the controlled bridge becomes unstable is significantly reduced. The lagging of the surfaces motion behind the pitching leads to instability.

As a simple solution, the application of the standard output gains designed for high wind speed may be sufficient. However, it must be remembered that such gains are truly optimal only at the design wind speed, and control performance may be very poor for different wind conditions. The control law, which is designed for a higher wind speed, utilizes the control surfaces excessively in the lower wind range.

The statement above can be noticed in Figure 6-13. In this case the wind blows at 9 m/s and the control is designed for a wind velocity much higher. In order to bring the structure to a stable state, excessive use of the moving surfaces is needed. This can be seen by the amplitudes of the wings rotations versus time, especially during the first seconds after the initial impulse.

Another possibility to control the real structure in low wind ranges if gains are calculated for a high design speed is to reduce the length of the wings. If the bridge span is, say, 2.000m, only a half or a third of the wing's length would be forced by the controllers to rotate.

A third possibility is to let the computer choose the best control law as a function of the wind speed, which can be read by Pitot tubes fixed to the deck. For example, for $U < 8$ m/s, the wings remain at rest; for $8 < U < 9$, gain is designed for $U_g = 9$ m/s; for $9 < U < 11$ gain is designed for $U_g = 11$ m/s; for $11 < U < 15$, gain is designed for $U_g = 15$ m/s; for $15 < U < 21$ m/s, gain is designed for $U_g = 19$ m/s. The fourth alternative is to adopt a variable-gain output feedback control, which is the subject of Chapter 7.